Heterogeneous Nonclassical Carbonyls Stabilized in Cu(I)- and Ag(I)-ZSM-5 Zeolites: Thermodynamic and Spectroscopic Features

5 AUTHORS, INCLUDING:

Carlo Lamberti
Università degli Studi di Torino

379 PUBLICATIONS **13,103** CITATIONS

SEE PROFILE

A. Zecchina
Università degli Studi di Torino

560 PUBLICATIONS **19,907** CITATIONS

SEE PROFILE

Heterogeneous Nonclassical Carbonyls Stabilized in Cu(I)− and Ag(I)−ZSM-5 Zeolites: Thermodynamic and Spectroscopic Features

Vera Bolis* and Alessia Barbaglia

DiSCAFF and NIS Centre of Excellence, Università Piemonte Orientale "A. Avogadro", Via Bovio 6, 28100 Novara, Italy, and INSTM Unità del Piemonte Orientale

Silvia Bordiga, Carlo Lamberti,* and Adriano Zecchina

Dipartimento di Chimica IFM and NIS Centre of Excellence, Università di Torino, Via P. Giuria 7, 10125 Torino, Italy, and INFM UdR di Torino Università, Torino, Italy

Received: January 28, 2004; In Final Form: April 16, 2004

A systematic analysis of the thermodynamic and spectroscopic features of a vast set of data on carbonyl-like complexes present in the literature, combined with some new experimental data here reported, allowed us to attempt to single out the electrostatic σ- and π-contributions in the formation of carbonyl bonding for the so-called "nonclassical carbonyls" hosted inside zeolitic nanocavities. In particular, the room-temperature adsorption of CO on well-defined Cu(I) and Ag(I)−ZSM-5 systems (as testified by X-ray absorption experiments) was studied by means of the joint use of IR spectroscopy and adsorption microcalorimetry. The formation in the zeolite pores of heterogeneous $[Cu(CO)_2]^+$ and $[Ag(CO)]^+$ complexes, the stoichiometry of which is in good agreement with the homogeneous nonclassical carbonyls, was monitored as a function of increasing p_{CO}. In the early stage of the interaction, strong and irreversibly bound monocarbonyl species characterized by $\tilde{\nu}_{CO_{ads}} > \tilde{\nu}_{CO_{gas}}$ are formed on Cu(I) and Ag(I) sites. Conversely, labile adducts (electrostatic in nature) are formed on Na^+ and K^+ sites hosted in the same zeolite pores. The zero-coverage enthalpy of CO adsorbed on Cu(I) and Ag(I) sites ($-\Delta_{ads}H \sim 120$ and ~ 100 kJ/mol, respectively) is much larger than the $-\Delta_{ads}H$ values measured for the two alkaline-metal adducts (~ 35 and ~ 28 kJ/mol for Na^+ and K^+, respectively), despite the closeness of the charge/radius ratios of the two sets of metal cations [Na^+ and Cu(I); K^+ and Ag(I)]. The high $-\Delta_{ads}H$ values and the irreversible nature of (a fraction) of the d-block metal carbonyls suggest the onset of a π-back-donation reinforcing the carbonyl bond with respect to a plain σ-coordination. A clear deviation from an empirical rule, which linearly correlate $\Delta\tilde{\nu}_{CO}$ and $-\Delta H_{ads}$ quantities for a large set of non-$d/d^0/d^{10}$ metal carbonyls, was observed in the case of copper-and silver−carbonyls, confirming the interplay of σ- and π-back-donation contributions for such species, otherwise defined nonclassical carbonyls. The $\Delta\tilde{\nu}_{CO}$ versus $-\Delta_{ads}H$ empirical rule was found of general validity, in that it allows to infer the enthalpy values from the blue-shift of the C−O stretching frequency (and vice-versa) in the case of non-d/d^0 metal carbonyls, whereas it allows to roughly estimate by the deviation from the line the extent of the π-back-donation in the case of d-block metal carbonyls. Further, the spectroscopic and thermodynamic features of carbonyl species formed on (partially) reduced copper sites have shown that in the absence of strong electrostatic plus σ-coordinative components the carbonyl bond is surprisingly weak, despite the presence of π-back-donation.

1. Introduction

Copper-exchanged molecular sieves have been widely investigated after the discovery that Cu−ZSM-5 are active in the direct decomposition of nitric oxide to nitrogen and oxygen.[1−3] Due to their superior catalytic activity, most of the data reported up to now refer to more than 100% copper-exchanged samples[4,5] prepared via a conventional ion exchange with aqueous solutions of cupric ions, which contain mixtures of copper ions in different aggregation and oxidation states.[1−3,6−10] The heterogeneity of copper species in catalysts prepared following this way is evident, and implies that a structural model for Cu cations cannot be confidently assessed. This makes the elucidation of structural

and catalytic properties of isolated and clustered species a difficult subject. Since the early 1990s our group has developed an ongoing research[11−23] in the characterization of Cu(I)−ZSM-5 samples prepared following an original exchange path, based on the reaction at 573 K between the zeolite (in the protonic form) and gaseous CuCl following the scheme:

$$Si(OH^+)Al^-_{(surf)} + CuCl_{(g)} \rightarrow Si(OCu^+)Al^-_{(surf)} + HCl_{(g)} \tag{1}$$
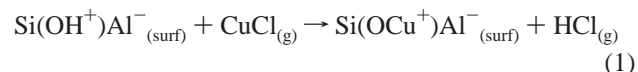
It has been proven that the so obtained material can be considered as a model solid, containing only well-defined isolated copper species in a single, well defined, oxidation state. Even if far away from the complex, structurally and chemically disordered "true-catalyst", Cu(I)−ZSM-5 prepared following our method has been of greatest help in understanding the local

* Corresponding authors. Prof. V. Bolis: tel, +39-0321-375-840; fax, +39-0321-375-821; e-mail, bolis@pharm.unipmn.it. Dr. C. Lamberti: tel, +39-011-6707841; fax, +39-011-6707858; e-mail, carlo.lamberti@unito.it.

Heterogeneous Nonclassical Carbonyls

J. Phys. Chem. B, Vol. 108, No. 28, 2004 **9971**

structure of Cu(I) ions in zeolites which certainly affects their catalytic behavior. In fact, because of its model character, the system offers clear and simple spectroscopic, energetic and structural outputs which assignment is straightforward. This is the reason the experimental results emerging from its characterization have been also used as model values for comparison of the computational outputs obtained in advanced quantum chemical studies.[24−29] It is finally worth recalling that this method having the advantage of directly introducing only Cu(I) cations was first applied to ZSM-5 matrix but was subsequently extended to faujasite,[20,30,31] Mordenite,[20,32] and β[20] molecular sieves. The straightforward introduction of the sole Cu(I) cations in the zeolites pores prevents the need of in vacuo high-temperature autoreduction of Cu(II) cations,[6−9,33] which could damage the structure of some zeolites.

Beside their interest as catalytic systems, zeolites are also of greatest interest in that their three-dimensionally organized microporous structure allows to stabilize in the nanocavities small metal clusters and otherwise labile coordination complexes.[14,16,17,22,23,34,35] Indeed, the zeolite framework has a "protective effect" on the intrazeolite heterogeneous adducts, not easily obtained in homogeneous conditions.[36−42] The high reactivity of such Cu(I) cations, which are able to bind N_2 molecules even at room temperature, has been explained in terms of a considerably high coordinative unsaturation.[14,15,22,43−46] Cu(I) cations are in fact able to form, depending on equilibrium pressure and temperature, nitrosyl and carbonyl complexes of high structural and spectroscopic quality that can be investigated in comparison with carbonyl complexes typical of homogeneous chemistry. In particular, in the case of CO, the Cu(I) cations hosted in the zeolite framework are able to form (even at room temperature) relatively stable adducts such as the mono-$[Cu(CO)]^+$ and dicarbonyl $[Cu(CO)_2]^+$ complexes[11,12,14−17,47,48] which evolve to tricarbonyl $[Cu(CO)_3]^+$ species when the temperature is lowered to $\approx$100 K.[11,12,14−17] These carbonyl-like species are characterized by a stability which depends on the conditions, but which discriminates at least two families of cationic sites.[5,6,14−17]

Beside our group, Kuroda and co-workers[6,44−46,49] have extensively studied the adsorption of CO on Cu-zeolites by means of the joint use of spectroscopic and calorimetric techniques. A remarkable difference between the results obtained by the Kuroda group and ourselves is that the former have typically studied over-exchanged copper systems obtained through conventional and original wet exchange procedure. This makes a straightforward comparison not always feasible.[50] Indeed the wet exchange procedure does necessarily involve the high-temperature autoreduction of Cu(II) cations and this fact implies the presence of a large heterogeneity of copper species, characterized by different coordination and oxidation states. In this respect, it is worth noticing that the principal aims persecuted by us and by Kuroda's group, along the ongoing research made in the past decade by both groups, are somehow different. The Kuroda's group has been mainly involved in the characterization of Cu−ZSM-5 systems as close as possible to the true, and thus intrinsically complex, catalysts.[43−46,49,51] On the other hand, in our group the efforts have been focused in the preparation and characterization of a model solid containing only isolated Cu(I) species resulting in spectroscopic and calorimetric data of straightforward interpretation. Such model solid is probably far away from the true catalyst investigated by Kuroda's group, but it allows to shed light on the fundamental interaction between Cu(I) and guest molecules such as CO. These considerations must be taken into account when

comparing the results obtained in the present work with those reported in the literature on over-exchanged samples.

As far as Ag-exchanged zeolites are concerned,[52,53] these systems are of greatest interest in several catalytic and photocatalytic processes, among them the photochemical dissociation of H_2O into H_2 and O_2,[54] the disproportionation of ethylbenzene,[55] and the photocatalytic decomposition of NO.[56] Opposite to what observed for copper-exchanged zeolites, for the silver ones, and in particular Ag(I)−ZSM-5 investigated also by Kuroda's group,[53] the comparison of the results obtained in the different laboratories is straightforward, thanks to the conventional wet exchange procedure generally adopted.

The aim of the present work is to investigate the room temperature interaction of CO with coordinatively unsaturated Cu(I) and Ag(I) cations hosted in ZSM-5 zeolites, to quantify the ability of the cations to form CO adducts, and thus to assess the Lewis acidic strength of the noble metal-exchanged zeolite. On the other hand, the RT adsorption of CO allows to investigate the nature and the stability of the carbonyl species formed, in view of finding a clue to single out the different contributions to the bonding of CO with d-block metals. The two cations under study have electronic similarities in that both Cu(I) and Ag(I) belong to group 11 (IB) of transition metals, and possess analogous valence shell electronic configuration ($3d^{10}$ and $4d^{10}$, respectively). The size of the two cations by contrast is significantly different, as witnessed by the values of the ionic radii of the two elements: r[Cu(I)] = 0.96 Å and r[Ag(I)] = 1.26 Å.[57] The two cations are expected to behave similarly, at least as far as a Lewis acid−base interaction is involved, but being the size of the two ions very different, the overlap of the metal and carbon monoxide orbitals in both σ- and π-components of the bond is expected to be different. In fact, both carbonyl and amino complexes formed at RT on Ag(I)−ZSM-5 show a stoichiometry lower than the stoichiometry of the adducts formed on Cu(I)−ZSM-5: $[Ag(CO)]^+$ versus $[Cu(CO)_2]^+$ and $[Ag(NH_3)_2]^+$ versus $[Cu(NH_3)_4]^+$, see refs 58, 59, and 16, respectively. The stoichiometry of such heterogeneous complexes is in good agreement with the one of the homogeneous chemistry complexes.[36−41] These differences can be, at least partially, explained from an electrostatic point of view, since the charge density of Cu(I) cations is much larger than in the case of Ag(I) cations.

To single out the electrostatic contribution to the whole interaction, the adsorption of CO on Na^+ and K^+ cations hosted in the same ZSM-5 microporous system was also investigated.[53,60−62] The two alkaline cations possess a charge/radius ratio very close to that of Cu(I) and Ag(I). Indeed, being the ionic radii of Na^+ and K^+ 0.97 and 1.33 Å,[57] respectively, the charge/radius ratio (i.e., the local electric field) of the former is 1.03 $|e|Å^{-1}$, whereas that of the latter is 0.75 $|e|Å^{-1}$. The two values compare well with the charge/radius ratios of Cu(I) and of Ag(I), which are 1.04 and 0.79 $|e|Å^{-1}$, respectively.

The room-temperature adsorption of CO was studied by means of the combined use of IR spectroscopy and adsorption microcalorimetry, to reveal the nature of the adspecies entrapped in the zeolite nanocavities, and to determine the stoichiometry of the adducts, as well as the energetic of their formation and their stability upon outgassing. The stabilization (in terms of energy of interaction) of the adducts formed as a consequence of the onset of the synergistic ($\sigma + \pi$) carbonyl bond was estimated.[16,36−42,53,63−65] EXAFS analysis was performed in order to check the local environment of noble metal cations in the zeolite cavities as well as to determine structural parameters needed for a better understanding of the nature of the species

formed in the adsorption processes investigated. XANES spectroscopy has been used as local probe of the geometrical and electronic rearrangements undergone by both Cu(I) and Ag(I) upon formation of Cu(I)(CO)$_n$ (n = 1, 2, 3), Cu(I)(CO)$_n$-(NH$_3$), and Ag(I)(CO)$_2$ complexes.[8,14,17,18,30,58,66] Finally, the ν_{CO} stretching frequency and the $-\Delta_{ads}H$ adsorption enthalpy values obtained have been discussed in comparison with data previously reported, concerning carbonyl-like species formed at the surface of solids containing metal cations either non-d or d^0/d^{10} in nature, for which the π-back-donation of d electrons was prevented.[53,60−63,67−69] A critical exam of the deviation in the case of d-block metal cations from the correlation existing between the spectroscopic and thermodynamic parameters observed for non-d systems has been made.

2. Experimental Section

2.1. Materials. Cu(I)- and Ag(I)−ZSM-5 zeolites have been prepared starting from the same NH$_4$−ZSM-5 precursor (Si/Al = 14, Polimeri Europa SpA, Centro Ricerche di Novara). As for the cuprous form of the material, the exchange procedure was done in two steps. First, ammonium ions were decomposed by a thermal treatment in vacuo at 673 K (6 h, $p \leq 10^{-3}$ Torr, 1 Torr = 133.3 Pa), yielding the H−ZSM-5 protonic form of the zeolite. Then the acidic proton was exchanged from the gas phase with CuCl. The sample was carefully handled in order to prevent oxidation of Cu(I) to Cu(II) species, as described in details elsewhere.[18]

In the case of Ag−ZSM-5, the Ag(I) cations were introduced through a conventional wet procedure employing an aqueous solution of AgNO$_3$. This sample too was carefully handled but in this case in order to prevent light exposure, so avoiding (as much as possible) photoreduction of Ag(I) species and consequent formation of [Ag$_n$]$^{x+}$ clusters.[70] In both Cu(I)− and Ag(I)−ZSM-5 samples a nearly total exchange of the protons of the parent material was achieved, as confirmed by IR spectroscopy. Indeed, the band of the O−H stretching mode of bridged Si−(OH)−Al groups typically located at ≈3610 cm^{-1} in the H−ZSM-5 precursor,[14] is virtually absent in the case of Cu(I)− and Ag(I)−ZSM-5 samples. This ensured that one Me(I) cation was present in the materials examined for every framework Al atom. By contrast, the high-frequency band at ≈3748 cm^{-1}, due to the OH stretching frequency of the external SiOH groups, was left virtually unaffected by the exchange procedure. For the IR spectra (not reported for the sake of brevity) see ref 58.

Na−ZSM-5 and K−ZSM-5 were obtained by a conventional wet exchange procedure (ref. [60]) by the same NH$_4$−ZSM-5 precursor as for Cu(I)− and Ag(I)−ZSM-5 samples. Also in these latter cases a complete proton-metal cation exchange was achieved.

2.2. Methods. Cu−K and Ag−K edge EXAFS and XANES spectra have been collected in transmission mode at the 6.0 GeV storage ring of the European Synchrotron Radiation Facility (ESRF, Grenoble, F): beamlines BM8 GILDA and BM29, respectively. We shall refer to refs 8 and 58 for a detailed description on the X-ray data collection and analysis at Cu−K and Ag−K edges, respectively. The experimental cell used to perform in situ X-ray absorption spectra has been described elsewhere.[71]

The heats of adsorption were measured at 303 K by means of a heat-flow microcalorimeter (Tian-Calvet type, Setaram-France) in order to evaluate the enthalpy changes related to the adsorption ($q^{diff} = -\Delta_{ads}H$). A well-established stepwise procedure, previously described[18,21,67,68,72] was followed. The

calorimeter was connected to a high vacuum ($p \leq 10^{-5}$ Torr) gas-volumetric glass apparatus, that enabled to determine in the same experiment the adsorbed amounts (Δn_{ads}) and the heats evolved (ΔQ^{int}) for small increments of the adsorptive. Thanks to the differential construction of the apparatus, all parasite effects other than the one due to the interaction of the gas with the solid surface were compensated. The adsorbed amounts ($n_{ads} = \Sigma\Delta n_{ads}$) and the integral heat evolved during the process ($Q^{int} = \Sigma\Delta Q^{int}$) will be reported (per gram of zeolite) at increasing equilibrium pressure of CO, up to ≈80−90 Torr, giving rise to the volumetric and calorimetric isotherms, respectively, the latter being reported in section C of the Supporting Information for brevity. The pressure was monitored by means of a transducer gauge (Barocel 0−100 Torr, Edwards). A first run of adsorption was performed on the samples previously outgassed at the chosen activation temperature (673 K for Cu(I)− and 400 K for Ag(I)−ZSM-5, 2 h at $p \leq 10^{-5}$ Torr). For Na- and K−ZSM-5 samples the same activation conditions as for Cu-(I)−ZSM-5 were adopted, thus ensuring the maximum degree of dehydration. A second run was performed after outgassing overnight (14 h) the sample at the calorimeter temperature, to evaluate the reversible (in the adopted conditions) component to the adsorption.

The adsorption of CO on Cu(I)−ZSM-5 zeolite previously contacted with NH$_3$ (up to $p_{NH3} \approx 90$ Torr) and subsequently outgassed at 303 K was also studied. In this latter case, Cu(I) sites do possess a reduced coordinative unsaturation with respect to the pristine sample, in that are already engaged in the stable (upon RT outgassing) amino [Cu(NH$_3$)$_n$]$^+$ adducts (with $2 \leq n \leq 1$).

For the IR spectroscopy measurements, thin self-supporting wafers of Cu(I)− and Ag(I)−ZSM-5 zeolites were prepared and activated by outgassing at the same temperature as for the volumetric-calorimetric experiments, under a dynamical vacuum of $p \sim 10^{-4}$ Torr, inside an IR cell specially designed to allow in situ high-temperature treatments and gas dosage, as well as low-temperature measurements.[11−18,60] The IR spectra were recorded at 2 cm^{-1} resolution on a BRUKER FTIR 66 spectrometer equipped with an HgCdTe cryodetector.

3. Results

3.1. Local Environment of Metal Sites as Probed by EXAFS. The EXAFS data analysis (see section A of the Supporting Information for more details), performed on the first shell filtered data using phases and amplitudes extracted from Cu$_2$O and Ag$_2$O model compounds, gave a metal−oxygen distance of 2.00 (±0.02) Å for Cu(I)−ZSM-5 and 2.30 (±0.03) Å for Ag(I)−ZSM-5. The corresponding coordination numbers were found to be 2.5 (±0.3) and 2.5 (±0.4), respectively. The difference observed in the metal−oxygen distances is clearly due to the difference in size of the two ions: (0.96 and 1.26 Å fir Cu(I) and Ag(I), respectively.[57] Conversely, the coordination numbers were found to be virtually the same (within experimental error) in the two cases. The (average) value of 2.5 for the coordination numbers is interpreted as due to the presence within the ZSM-5 zeolite of both two-coordinated and three-coordinated extraframework cations, in a nearly equal proportion. Exposure to CO gas (dotted line curves in Figure A of the Supporting Information) strongly modifies the EXAFS spectra, indicating that a strong metal−carbonyl interaction does occur. The structure of [Cu(CO)$_2$]$^+$ complexes measured in situ at room temperature is discussed in section B of the Supporting Information, where a multiple scattering approach has been adopted.[73] The obtained results can be summarized as follows:

Heterogeneous Nonclassical Carbonyls

J. Phys. Chem. B, Vol. 108, No. 28, 2004 **9973**
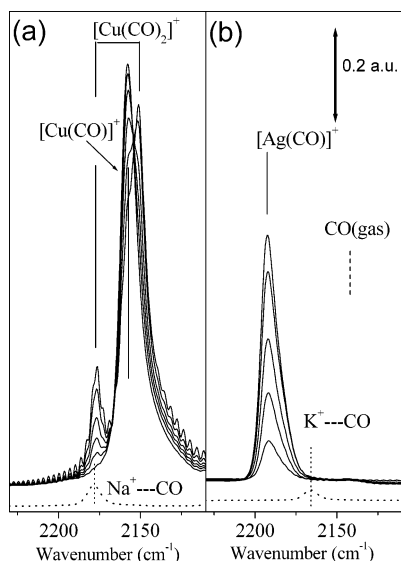
Figure 1. Part (a) IR spectra of CO adsorbed at RT on Cu(I)−ZSM-5 at increasing p_{CO} (top curves) and on Na−ZSM-5 (bottom curve, highest p_{CO} only). Vertical solid and dotted lines refer to the position of copper and sodium carbonyl species, respectively. Part (b) as part (a) for Ag(I)−ZSM-5 (top curves) and K−ZSM-5 (bottom curve). Vertical solid and dotted lines refer to the position of silver and potassium carbonyl species, respectively. Dashed line refers to the unperturbed CO molecule.

the experimental EXAFS signal has been reproduced by adding the contribution of 2.3 ± 0.3 oxygen framework atoms located at 2.11 ± 0.03 Å to that of 1.8 ± 0.3 CO molecules. The Cu−C distance obtained for the $[Cu(CO)_2]^+$ complex is 1.88 ± 0.02 Å, the C−O distance is 1.12 ± 0.03 Å, and the Cu−C−O bond angle is linear within the error bars ($170° \pm 10°$), in agreement with indirect IR evidence (vide infra). The number of coordinated CO molecules (1.8 ± 0.3) is in agreement with the $[Cu(CO)_2]^+$ stoichiometry suggested by IR and microcalorimetry (vide infra).

3.2. Nature of the Carbonyl-like Complexes As Revealed by IR and XANES. In Figure 1a the room-temperature IR spectra (2000−2200 cm^{-1} region) of CO adsorbed on Cu(I)−ZSM-5 (top curves) and on Na−ZSM-5 (bottom dashed curve) are reported. In the case of Cu(I)−ZSM-5, the spectra are reported at increasing CO equilibrium pressure (p_{CO}), while only the highest p_{CO} spectrum is reported for the Na−ZSM-5 case. The early contact of Cu(I)−ZSM-5 with CO yields to the formation of $[Cu(CO)]^+$ species, (band at 2157 cm^{-1}),[12,14−17,47] which saturates very quickly, as suggested by the gradual decrease of its intensity starting from $p_{CO} \approx 0.1$ Torr. From this p_{CO} onward, the monocarbonyl species do evolve to dicarbonyl, as witnessed by the appearance of the symmetric and asymmetric modes of the $[Cu(CO)_2]^+$ complex (bands at 2178 and 2151 cm^{-1}, respectively). The $[Cu(CO)]^+ \rightarrow [Cu(CO)_2]^+$ evolution upon increasing p_{CO}, is confirmed by the presence of two well-defined isosbestic points at 2166 and 2154 cm^{-1}.[12,14−17,47] The little intense band located at 2178 cm^{-1}, shown in the bottom of the Figure 1a, is due to the stretching mode of the Na$^+\cdots$CO electrostatic adducts formed upon exposure of Na−ZSM-5 zeolite to the gas.[60]

Two important features must be noticed: (i) the upwards shift of the $\tilde{\nu}_{CO}$ stretching frequency with respect to the CO gas ($\tilde{\nu}_{CO}$ = 2143 cm^{-1}) is significantly higher for Na$^+\cdots$CO adducts than for $[Cu(CO)]^+$ species ($\Delta\tilde{\nu}$ = +35 against +14 cm^{-1}), despite the virtually identical charge/ionic radius ratio of the two cations; (ii) the adspecies formed on Na$^+$ sites are labile and easily eliminated by reducing p_{CO}, whereas the adspecies formed on

Cu(I) sites are at least partially stable upon evacuation at RT. In particular, the spectroscopic evidence suggests that while the dicarbonyl species are completely destroyed upon outgassing, a significant fraction of monocarbonyl species does resist to the evacuation (in the adopted conditions).

In Figure 1b, the IR spectra of CO adsorbed on Ag(I)−ZSM-5 (top curves) and on K−ZSM-5 (bottom curve) are reported. In the case of the Ag−zeolite, the spectra are reported also at increasing p_{CO}. The band observed at 2192 cm^{-1} is due to the C−O stretching of the $[Ag(CO)]^+$ species formed.[53,58] The weak band of CO adsorbed on K−ZSM-5 centered at 2166 cm^{-1} is readily assigned to the formation of K$^+\cdots$CO electrostatic adducts.[60]

Again, by comparing the spectroscopic features of Ag(I)− and K−ZSM-5 systems, two important features must be noticed: (i) the upwards shift of the $\tilde{\nu}_{CO}$ stretching frequency with respect to the ν_{CO} of the gas is again different for the two systems despite the nominal identical charge/ionic radius ratio of the two cations; (ii) opposite to what observed for the Cu-(I)/Na$^+$ pair, the upward shift is much larger for the transition metal than for the alkaline cation ($\Delta\tilde{\nu}$ = +49 cm^{-1} for Ag(I) and +23 cm^{-1} for K$^+$); (iii) the adspecies formed on K−ZSM-5 sites are labile (in that they are completely eliminated by evacuation at RT, as for Na−ZSM-5), whereas the monocarbonyl species formed on Ag(I)−ZSM-5 sites are much more stable (only a part of them are removed by evacuation at RT).

Figure 2a reports the XANES spectra of Cu(I)−ZSM-5 before and after interaction with CO (p_{CO} = 40 Torr) at RT (dotted and full lines respectively). For comparison also the XANES spectrum of Cu metal (dashed line) is reported. The XANES spectrum of Cu−ZSM-5 is typical of Cu(I) species, exhibits the 1s $\rightarrow$ 4p$_{xy}$ electronic transition at 8983.5 while, upon formation of $[Cu(CO)_2]^+$ complex, the 1s $\rightarrow$ 4p$_{xy}$ electronic transition is reduced in intensity and undergoes a red shift of 1.1 eV, giving a response which is intermediate between Cu(I) and Cu(0) species.[6,14,17,18,22,23] This fact is even more evident in the derivative spectra reported in part b of the Figure and reflects a decrease of the actual charge density on the cation as a consequence of the coordination of two CO molecules.

Parts c and d of Figure 2 report the same data for the Ag-(I)−ZSM-5 system. Due to the shorter lifetime of the 1s core-hole in Ag (with respect to Cu), the XANES features at the Ag K-edge are intrinsically less resolved. Nevertheless the K-edge of Ag(I)−ZSM-5 in vacuo occurs at a definitely higher energy than that of Ag metal, testifying the cationic nature of silver species hosted in the zeolite. We are however unable to evidence a significant edge shift upon interaction with CO. This can be due to either a less pronounced ability of Ag(I) to receive charge density, or to an insufficient energy resolution of the XANES spectra, or to both effects. However, the formation of silver−carbonyl adducts strongly perturbs the near-edge structure witnessing a change in the electronic configuration of Ag(I) cations.[53]
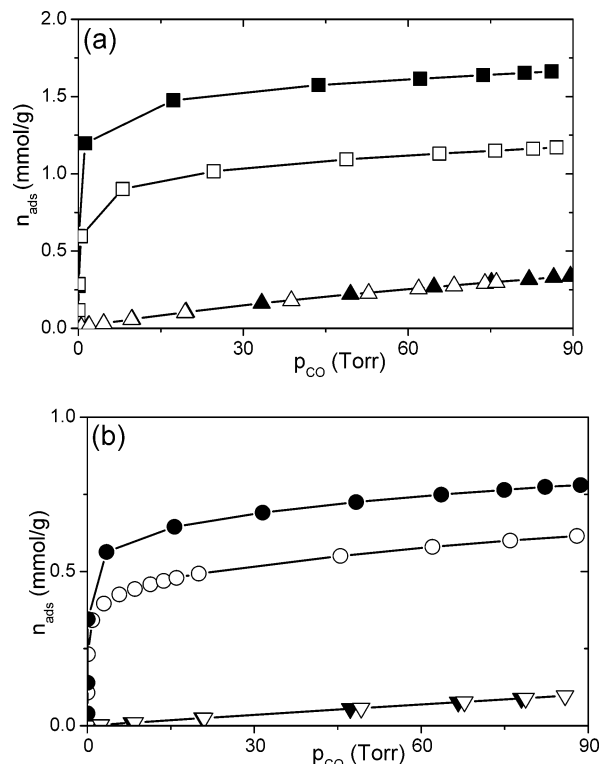
3.3. Stoichiometry of the Carbonyl-like Complexes, by Adsorption Microcalorimetry. *3.3.1. Cu(I) and Na$^+$ Cases.* In Figure 3a the volumetric isotherms of CO adsorbed on Cu-(I)− and Na−ZSM-5 zeolites are reported. For the corresponding calorimetric isotherm, please see part a of Figure C in the Supporting Information. It is clearly evident that CO interacts with Cu(I)−ZSM-5 zeolite strongly and with a large irreversible component, as witnessed by the initial absence of an equilibrium pressure and by the noncoincidence of the first and second runs of adsorption. By contrast, the interaction of CO with Na$^+$ sites is pressure-dependent since the early stages of the process, and
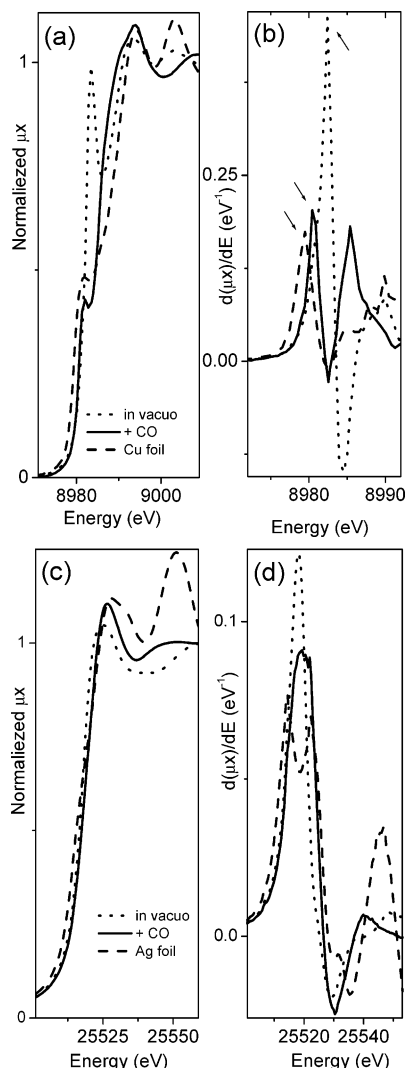
Figure 2. Part (a): normalized XANES spectra of Cu metal reference sample (dashed line) and of Cu(I)−ZSM-5 before and after interaction with CO, dotted and solid lines, respectively. Part (b): first derivative of the spectra reported in part (a). Parts (c) and (d) as parts (a) and (b) for Ag metal foil and Ag(I)−ZSM-5.

Figure 3. Part (a): volumetric isotherms (n_{ads} vs p_{CO}) of CO adsorbed at 303 K on Cu(I)−ZSM-5 (squares) and on Na−ZSM-5 (up triangles). Solid symbol, total adsorption (first run); open symbols, reversible adsorption (second run). Part (b) as part (a) of CO adsorbed on Ag(I)−ZSM-5 (circles) and on K−ZSM-5 (down triangles).

TABLE 1: Quantitative and Energetic Data of the Adsorption ($T_{ads} = 303$ K) of CO on Cu(I)− and Ag(I)−ZSM-5, in Comparison with Na− and K−ZSM-5 ($p_{CO} = 90$ Torr)

sample	$n_{ads}{}^a$ (mmol/g)	CO molecules per cation	$Q^{int\ b}$ (J/g)	$[q_p]^{mol} = (Q^{int}/n_{ads})_p{}^c$ (kJ/mol)
Cu(I)−ZSM-5 first run (total ads)	1.68	2	126.7	75
Cu(I)−ZSM-5 second run (reversible ads)	1.18	1.5	75.04	64
Cu(I)−ZSM-5 (first − second) (irreversible ads)	0.50	0.5	51.66	103
Na−ZSM-5 first − second run (reversible ads)	0.34	0.4	11.82	35
Ag(I)−ZSM-5 first run (total ads)	0.78	1	52.74	67
Ag(I)−ZSM-5 second run (reversible ads)	0.62	0.8	37.38	60
Ag(I)−ZSM-5 (first − second) (irreversible ads)	0.16	0.2	15.36	96
K−ZSM-5 first − second run (reversible ads)	0.10	0.1	2.90	28

^{a} n_{ads} (mmol/g), adsorbed amounts per gram of zeolite. ^{b} Q^{int} (J/g), integral heat of adsorption per gram of zeolite. ^{c} $[q_p]^{mol}$ (kJ/mol) = ($Q^{int}/n_{ads})_p$, integral molar heat of adsorption at $p_{CO} = p$.

the first and second runs isotherms are virtually identical in the whole equilibrium pressure interval examined (0−90 Torr). The irreversible process observed in the case of Cu(I)−ZSM-5 zeolite is virtually complete at $p_{CO} < 10$ Torr, in that at higher p_{CO}, the first and second runs isotherms lie parallel. The difference between the amount CO adsorbed per gram of zeolite in Cu(I)− and Na−ZSM-5 is striking: the total amount of CO adsorbed on Cu(I)−ZSM-5 is about 5 times the amount adsorbed on Na−ZSM-5 (first run). The same holds for the reversible component too, being more than three times greater than that observed on Na−ZSM-5 (first and second runs). The trend of the calorimetric isotherms (see part a of Figure C in the Supporting Information) is quite similar to that of the volumetric isotherms. The integral heat evolved at $p_{CO} = 90$ Torr on Cu-(I)−ZSM-5 is about 10 times the correspondent quantity on Na−ZSM-5 for the total adsorption (first run) and about six times for the reversible adsorption (second run). This datum indicates that not only the amounts adsorbed on copper- are much larger than on sodium-exchanged zeolite, but also that the CO adducts formed in the two systems (including the second run labile species) are different in nature and are much more energetic in the case of the transition metal cation. The quantitative and energetic data at a CO pressure of 90 Torr are reported in Table

1. The adsorbed amounts are reported as mmol of CO per gram of zeolite (n_{ads}) and also as a number of CO molecules per M(I) cation, to estimate the stoichiometry of the adducts formed. The heats of adsorption are reported as integral heat evolved per

Heterogeneous Nonclassical Carbonyls

J. Phys. Chem. B, Vol. 108, No. 28, 2004 **9975**

gram of zeolite (Q^{int}), as well as molar heat defined as $[q^{mol}]_p = (Q^{int}/n_{ads})_p$, i.e. the integral heat of adsorption normalized to the CO uptake at a given equilibrium pressure.[74]

At the highest p_{CO} reached, the number of CO molecules adsorbed per Cu(I) cation is close to two, indicating that the stoichiometry of the adducts is compatible with the $[Cu(CO)_2]^+$ formula, in agreement with the IR evidence (see Figure 1a) and with the EXAFS analysis (section B of the Supporting Information). By subtracting the second run isotherm from the first one it has been possible to quantify the fraction of the CO species stable to the pumping off, which turns out to be ∼30% of the total amounts adsorbed. The number of CO molecules reversibly adsorbed per Cu(I) cation is close to 1.5, and thus ∼0.5 molecules of CO are tightly (irreversibly in the adopted conditions) bound to the Cu(I) sites. This result suggests that all copper cations in average are involved in the formation of mono- and di-carbonyl-like species, and that only 50% are able to hold a CO molecule even upon outgassing (in the adopted conditions).

On the other hand, the number of CO molecules adsorbed per Na$^+$ is close to 0.4 (at the highest p_{CO} reached), revealing that only less than half of the total sodium cations hosted in the zeolite framework are able to create an electrostatic field sufficiently high to polarize CO molecules at RT. This result is compatible with the weakness of the interaction: the Na$^+$⋯CO species formed at RT are easily desorbed upon outgassing in agreement with the low heat of formation of the adducts (the molar heat of adsorption is $[q^{mol}]_{90} = 35$ kJ/mol).

In harmony with the higher stability of the CO species observed in the case of Cu(I)−ZSM-5, the average molar enthalpy of adsorption (at $p_{CO} = 90$ Torr) is $[q^{mol}]_{90} = 75$ kJ/mol for the total adsorption and $[q^{mol}]_{90} = 64$ kJ/mol for the secondary (reversible) one. The estimated average molar heat of formation of the irreversible monocarbonyl species is much higher: $[q^{mol}]_{90} \sim 103$ kJ/mol (see Table 1). These values confirm that the CO molecules bound to Cu(I) hosted in the zeolite framework originate carbonyl-like chemical bonds analogous to that of the complexes formed in homogeneous conditions. This statement is also supported by the observation that the $\tilde{\nu}_{CO}$ stretching frequency is too low (2157 cm^{-1}) to be simply interpreted on the basis of an electrostatic interaction plus a plain σ-coordination.

3.3.2. Ag(I) and K$^+$ Cases. In Figure 3b the volumetric isotherms of CO adsorbed on Ag(I)− and K−ZSM-5 zeolites are reported. For the corresponding calorimetric isotherm, please see part b of Figure C in the Supporting Information. Similarly to what observed for Cu(I)− and Na−ZSM-5 systems (Figure 3a), it is clearly evident that the interaction of CO with the transition metal zeolite is different in nature from that of the alkaline metal one. Indeed, the shape of the isotherms indicates that in the early stage of the process a most energetic, irreversible and pressure-independent adsorption occurs on Ag(I) sites, whereas a low energetic, fully reversible and pressure-dependent process occurs on K$^+$ sites. Further, by the inspection of the calorimetric isotherms (see Figure C in the Supporting Information), it is evident that the energy of interaction in the case of silver (in both total and reversible processes) is quite high with respect to potassium. The quantitative and energetic data are reported in Table 1, in comparison with those reported for Cu(I)− and Na−ZSM-5.

The amounts adsorbed at $p_{CO} = 90$ Torr on Ag(I)−ZSM-5 is much lower (ca. one-half) than the amounts adsorbed on Cu(I)−ZSM-5. By normalizing the adsorbed amounts to the number of Ag(I) cations, it was found that the number of CO molecules adsorbed at the Ag(I) sites is close to 1. This is in agreement with the IR evidence of the formation of the sole $[Ag(CO)]^+$ species (see Figure 1b). By subtracting the second run from the first run isotherm, it turns out that ∼20% of these species are stable upon outgassing at RT.

Again, both CO coverage reached and heat evolved (at $p_{CO} = 90$ Torr), in the case of the alkaline metal zeolite of reference, are quite low with respect to Ag(I)−ZSM-5. The number of CO molecules adsorbed per K$^+$ cation is indeed close to 0.1. This means that only ca. 10% of the total potassium sites (against ca. 40% of the sodium ones) are able to coordinate CO. The low coverage reached in the potassium case is clearly a consequence of the lower electrostatic field of the site which results in a lower polarization the CO molecules. The influence of the different alkaline cations charge density (0.75 and 1.03 $|e|Å^{-1}$ for K$^+$ and Na$^+$, respectively) is straightforward. In harmony with the very low measured heat of adsorption (∼28 kJ mol^{-1}, see Table 1), all CO species formed on K−ZSM-5 sites are easily eliminated upon evacuation at room temperature.

As in the case of Cu− and Na−zeolites discussed above, the average molar enthalpy of adsorption values confirm that in the case of the transition metal the interaction is much stronger than in the alkaline one ($[q^{mol}]_{90} = 67$ for Ag(I)− against 28 kJ/mol for K−ZSM-5, first run). The molar enthalpy of the second run is still quite high ($[q^{mol}]_{90} = 60$ kJ/mol), indicating that also the reversible fraction of $[Ag(CO)]^+$ species involves a relatively strong Lewis acid−base interaction. The average molar enthalpy of adsorption $[q^{mol}]_{90}$ for the irreversible component is estimated ∼96 kJ/mol (very close to the 103 kJ/mol value estimated for Cu(I)−ZSM-5).

3.4. Heat of Formation of the Carbonyl-like Complexes by Adsorption Microcalorimetry. To better describe the energetic of the formation of the carbonyl species we will now consider the evolution of the heat of adsorption (both integral and differential) with the increasing coverage. In Figure 4 the differential heat of adsorption of CO on Cu(I)− and Na−ZSM-5 (part a) and on Ag(I)− and K−ZSM-5 (part b) are reported versus the CO uptake. The differential heat values (experimental points) have been obtained by taking the middle points of the experimental histogram of the partial molar heats ($\Delta Q^{int}/\Delta n_{ads}$, kJ/mol) for incremental doses of the adsorptive as a function of the adsorbed amounts, n_{ads}.[18,21,75−78] The differential heat of adsorption ($q^{diff} = -\Delta_{ads}H$) is, however, more properly defined as the derivative of the curves of the integral heats as a function of the adsorbed amounts,[18,49,53,72,77−80] which are reported in the inset of Figure 4a,b (in both Cu(I)− and Ag(I)−ZSM-5 cases the integral heats curves were reasonably fitted by a polynomial of order five). Thus, in Figure 4a,b, beside the experimental points of the experimental histogram, the analytical derivative of the polynomial curve of the integral heats are also reported. A reasonably good agreement exists between the two methods over the whole adsorption range. In both Cu(I)− and Ag(I)−ZSM-5 cases, the integral as well as the differential enthalpy of adsorption strongly depends on surface coverage, suggesting either the presence of heterogeneous sites, or the heterogeneity of the species formed.[81] For most purposes, it is convenient to define the zero-coverage enthalpy of adsorption ($[q^{diff}]_0 = -[\Delta_{ads}H]_0$), which corresponds to the highest energy of interaction of the probe with the strongest sites. This datum is estimated by extrapolating the q^{diff} versus n_{ads} plots to vanishing coverage. The values estimated for the first run are $[q^{diff}]_0 \sim 120$ and ∼100 kJ/mol for Cu(I) and for Ag(I) sites, respectively. The value for the early formation of the reversible carbonyl-like species (second run) is lower ($[q^{diff}]_0 \sim 90$ kJ/mol) and very close for

TABLE 2: Spectral, Quantitative and Energetic Features of CO Adsorbed on Metal-Exchanged ZSM-5 Zeolites[a]

cationic site	p_{CO}, Torr	CO molecules per cation	$\tilde{\nu}_{CO}$, cm^{-1}	$(\tilde{\nu}_{CO})$, cm^{-1}	$(-\Delta H_{ads})_0$, kJ/mol	charge/radius, $|e|\text{Å}^{-1}$	carbonyl species
Cu(I)	<1	1.0	2157	+14	≥100	1.04	$[Cu(CO)]^+$
Cu(I)	1−90	2.0	2178 symm 2151 asymm	+21.5	≤90	≤1.04	$[Cu(CO)_2]^+$
Na$^+$	0−90	0.4	2178	+35	35	1.03	Na$^+$−CO
Ag(I)	0−90	1.0	2192	+49	100	0.79	$[Ag(CO)]^+$
K$^+$	0−90	0.1	2166	+23	28	0.75	K$^+$−CO
$[Cu(NH_3)_n]^+$ $n = 1, 2$	0−90	1.0	2100	−43	80	<1.04	$[Cu(NH_3)_n(CO)]^+$ $n = 1, 2$

[a] The Cu−ZSM-5 case is split into two rows to consider the formation of mono- and dicarbonyl species. In the latter case, the $\Delta\tilde{\nu}_{CO}$ shift has been computed using the average frequency of the symmetric and asymmetric stretching modes.
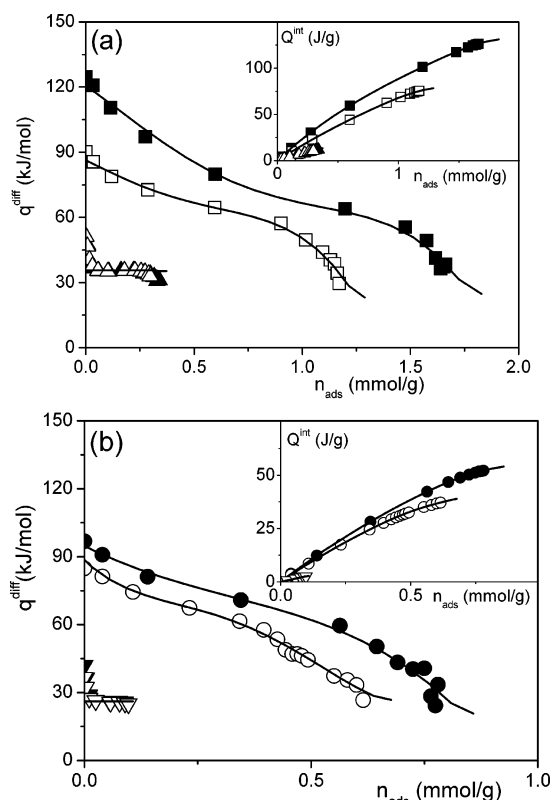
Figure 4. Part (a): differential heats of adsorption (q^{diff}) as a function of CO uptake (n_{ads}) for Cu(I)−ZSM-5 (squares) and Na−ZSM-5 (up triangles). Solid symbols, total adsorption (first run); open symbols, reversible adsorption (second run). Inset: integral heats of adsorption (Q^{int}) as a function of CO uptake (n_{ads}). Part (b): differential heats of adsorption (q^{diff}) as a function of CO uptake (n_{ads}) for Ag(I)−ZSM-5 (circles) and K−ZSM-5 (down triangles). Solid symbol, total adsorption (first run); open symbols, reversible adsorption (second run). Inset: integral heats of adsorption (Q^{int}) as a function of CO uptake (n_{ads}).

the two systems. As far as the coverage increases, the heat decreases to values typical of more labile species[67] and eventually fall down to values as low as ∼35 kJ/mol and ∼25 kJ/mol, for Cu(I)− and Ag(I)−ZSM-5, respectively. These latter values can be ascribed to a nonspecific interaction of CO with the walls of the micropores of the zeolite framework.[18,82,83] It is worth of noting that, even if nonspecific, the interaction of CO with the walls of the micropores involves an energy of interaction much higher than the latent heat of liquefaction of CO ($q_L = 6.7$ kJ/mol).

In the case of Na− and K−ZSM-5 systems the Q^{int} versus n_{ads} curves can be reasonably well fitted by a linear equation, giving rise to a constant differential heat (35 and 28 kJ/mol, respectively). In both cases, however, at low coverage the middle points of the experimental histogram do remarkably deviate from the constant value, indicating heterogeneity among the sites.

The same holds at high coverage. Despite this evidence, the linear fit of the integral heat curves seems to be the most realistic and reasonable for our purposes. Indeed, the apparent initial heterogeneity is likely due to the presence of a few defective centers (1−2% of the total active sites) interacting with CO more strongly than the alkaline metal cations. Similar experiments performed on the Al-free (and thus cation free) MFI-silicalite resulted in zero-coverage q^{diff} values giving similar evidence.[72] At high coverage the heat values measured progressively decrease at values lower than 35 (or 28) kJ/mol, similarly to what happens for the Cu(I)− and Ag(I)−ZSM-5 cases (vide supra). Again, these low heat values correspond to a process not involving a specific Me$^+$···CO interaction and must be disregarded in evaluating the enthalpy of formation of the adducts. It is also worth of noticing that the linear fit of the integral heat curves for the alkaline-metal zeolites is compatible with the fact that the relevant volumetric isotherms obey satisfactorily the Langmuir model,[84] which implies an ideal homogeneous collection of non interacting sites. Table 2 summarizes the spectral, quantitative, and energetic features of CO adsorbed on metal exchanged ZSM-5 zeolites investigated in the present work, including the values related to $[Cu(NH_3)_n(CO)]^+$ ($n = 1, 2$) complexes, which will be discussed in the next section.

3.5. Formation of Mixed Amino-Carbonyl Complexes. In Figure 5a the heat of adsorption of CO on Cu(I)−ZSM-5 precontacted at 303 K with NH$_3$ ($p_{NH3} \sim 90$ Torr) and subsequently evacuated at the same temperature is reported as a function of the adsorbed amounts. The RT pumping off was performed in order to get rid of the most labile amino-complexes.[16,18,21] This results in a distribution of $[Cu(NH_3)_2]^+$ and $[Cu(NH_3)]^+$ complexes which are still able to bind a CO ligand. In the figure the experimental points are reported together with the differential heats curves, obtained by differentiating the correspondent Q^{int} versus n_{ads} curves (interpolated by a polynomial of order three, but not reported for the sake of brevity). In the inset of the figure the amounts of CO adsorbed on the $[Cu(NH_3)_n]^+$ ($n = 1, 2$) species entrapped in the zeolite cavities are reported as a function of p_{CO} and compared to the amounts adsorbed on the bare Cu(I) sites (first run, see Figure 3a). The amounts of CO adsorbed on the sample containing the $[Cu(NH_3)_n]^+$ adducts are dramatically lower than the amounts adsorbed on the bare Cu(I) cations, particularly at the very early stage of the process (see inset). At $p_{CO} < 5$ Torr the CO uptake on the zeolite pre-contacted with NH$_3$ is about 10 times lower than on the activated one, whereas at $p_{CO} > 5$ Torr the uptake is only about three times lower. At $p_{CO} \geq 20$ Torr the two isotherms lye virtually parallel, indicating that at this stage of the process any phenomena significantly different in the two samples have been already accomplished. From this value of pressure onward, the difference between the amounts

Heterogeneous Nonclassical Carbonyls

J. Phys. Chem. B, Vol. 108, No. 28, 2004 **9977**
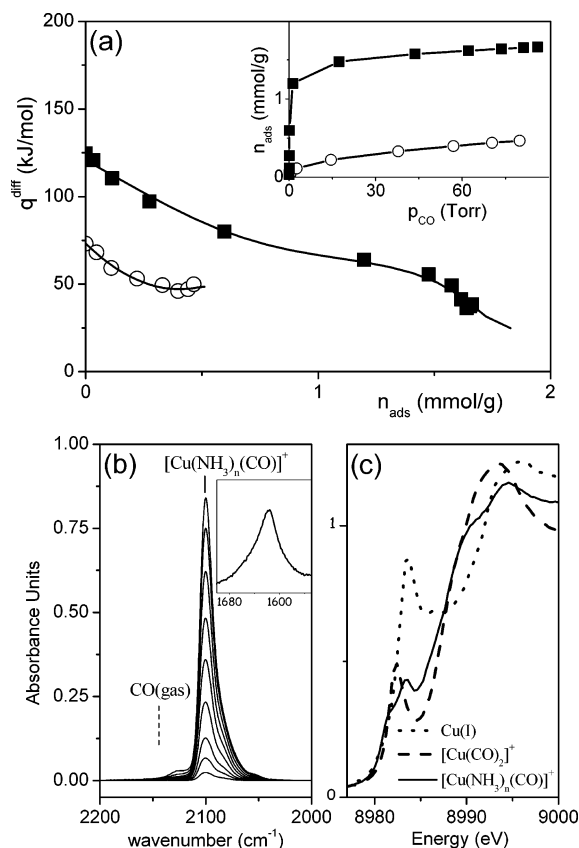
Figure 5. Part (a): differential heats of adsorption (q^{diff}) as a function of CO uptake (n_{ads}) for Cu(I)−ZSM-5 activated at 673 K (circle, first run), contacted with NH_3 at 303 K ($p_{NH_3} \approx 90$ Torr) and subsequently outgassed at 303 K in order to eliminate only the labile component of the copper amino-complexes. The differential heat of adsorption curve of CO on the bare (i.e., activated at 673 K) Cu(I) sites (square; see Figure 1b) is reported for comparison. Inset: correspondent volumetric isotherms of CO adsorbed on the samples as described for the heat curves. Part (b): IR spectra of CO adsorbed at RT at increasing p_{CO} (up to ≈ 20 Torr) on Cu(I)−ZSM-5 activated at 673 K, precontacted with NH_3 ($p_{NH_3} \approx 90$ Torr) and subsequently outgassed as described in part b. In the inset the $\delta(NH)$ bending mode of NH_3 bound to Cu(I) sites is reported (this band is not affected by increasing p_{CO}). Part (c): normalized XANES spectra of Cu(I)−ZSM-5 in vacuo (dotted line), after interaction with CO on both activated (dashed line) and previously contacted with NH_3 (solid line) samples.

of CO adsorbed on the two systems is ∼1.2 mmol/g, corresponding to ∼1 molecule of CO per Cu(I) cation, reflecting the formation of $[Cu(CO)_2]^+$ in the original sample and of $[Cu(NH_3)_n(CO)]^+$ ($n = 1, 2$) complexes in the sample pre-contacted with ammonia. The calorimetric isotherms (not reported for the sake of brevity) exhibit the same trend. The $[q^{diff}]_0$ for the CO adsorbed on the sample containing the amino-complexes is ∼75 kJ/mol, much lower than the ∼120 kJ/mol obtained for the bare Cu(I) cations. The curve of the differential heat of adsorption versus coverage decreases from the initial value down to q^{diff} ∼ 45 kJ/mol. This value, which corresponds to the differential heat of adsorption measured at the highest coverage attained ($p_{CO} \sim 90$ Torr) is significantly higher for the zeolite containing the copper-amino species entrapped in the nanocavities than in the pristine Cu(I)−ZSM-5 zeolite ($q^{diff} \sim 35$ kJ/mol, respectively).

In Figure 5b the IR spectra of CO adsorbed at room temperature on the sample containing the $[Cu(NH_3)_n]^+$ ($n = 1, 2$) species are shown. The spectra are characterized by a single well-defined component at 2100 cm^{-1}, which does not evolve upon increasing p_{CO} into the doublet typical of dicarbonyl

species, a feature which well agrees with the volumetric datum (Table 2). This datum indicates that the reduced coordinative unsaturation of the Cu(I) cations involved in the amino-adducts does affect significantly the ability of the sites to bind CO yielding to the formation of mono-carbonyl adducts only. Insertion of CO on the $[Cu(NH_3)_n]^+$ ($n = 1, 2$) species is not accompanied by a ligand displacement phenomenon, as testified by the invariance of the $\delta(NH)$ mode (1616 cm^{-1} see inset in Figure 5b) upon increasing p_{CO}.

The frequency of the C−O stretching mode of the $[Cu(NH_3)_n(CO)]^+$ complexes (2100 cm^{-1}) is dramatically lower than the $\tilde{\nu}_{CO}$ observed for the bare Cu(I) cations (2157 cm^{-1}, see Figure 1a), and even significantly lower than the $\tilde{\nu}_{CO}$ of the gas. This datum indicates that, in $[Cu(NH_3)_n(CO)]^+$ complexes, the π-back-donation dominates on both electrostatic and σ-donation components. The charge releasing character of the amino ligand plays certainly a role in quenching the electrostatic component of the Cu(I)←CO interaction.

In this regard, the XANES spectrum of the $[Cu(NH_3)_n(CO)]^+$ complexes hosted in ZSM-5 zeolite (solid line in Figure 5c) shows a significant red shift of both edge and pre-edge features with respect of the Cu(I)−ZSM-5 in vacuo (dotted line). XANES data confirm the strong charge releasing character of the amino ligand and explains the low $\tilde{\nu}_{CO}$ observed in the IR experiment. These results indicate that the preadsorption of ammonia does affect significantly the ability of the Cu(I) cations to bind CO yielding carbonyl-like species of different features and stability.

4. Discussion

4.1. Brief Overview on the Metal−CO Cations Interaction.

The literature on metal carbonyls is enormous, and it is out of the aims of this paper to treat this subject in an exhaustive way. We refer only to a few very recent and complete reviews by Willner and Aubke,[39] by Lupinetti et al.[40] and by Xu[42] and to the much more concise, but focalized on silver and copper carbonyls ones, by Strauss.[41]

The way CO interacts with metal cations may involve different contributions, according to the nature of the metal-cations sites. (i) The electric field created by a positive charge (like for instance an alkaline metal cation) causes a polarization of the CO molecule which depends on the local electric field of the site, i.e., on the charge density of the cation.[60,61] The spectroscopic evidence of the polarization of the molecule is an upward shift (blue-shift) of the stretching frequency of the C−O bond with respect to the $\tilde{\nu}(CO)$ of the gas (2143 cm^{-1}), owing to the increase of the force constant of the C−O bond, and the decrease of the bond length.[39−42,61b,61c] (ii) In the presence of an acceptor of electron pairs, such as a metal cation possessing empty orbitals of suitable energy (and thus acting as Lewis acidic center), the C-end lone pair of CO is transferred to the metal cation giving rise to a σ-coordination (M^{n+}←CO). In this case too, the interaction between CO and the metal cation causes the ν_{CO} stretching frequency to shift toward a value higher than that of the gas. It is generally accepted that the higher is the blue-shift, the stronger is the interaction, according to the Lewis acidic strength of the metal site.[39−42,60,61,67,68] (iii) In the case of transition metal cations possessing partially filled d orbitals, a significant M^{n+} → CO π-donation can occur from the orbitals of the d-block metal back to the orbitals of the CO molecule. The increase of the electronic density in the anti-bonding orbitals of the CO molecule causes the force constant of the C−O bond to decrease, the C−O bond length to increase and thus the $\tilde{\nu}_{CO}$ to be red-shifted with respect that of the gas.

The strength of the bond between CO and the *d*-block metal cations, and the $\tilde{\nu}_{CO}$ stretching frequency, are not expected in such a case to be simply correlated. In fact, as far as the strength of the carbonyl bond increases, as a consequence of the synergistic effect of the σ-($M^{n+}\leftarrow CO$) and π-($M^{n+}\rightarrow CO$) components, the resulting $\tilde{\nu}_{CO}$ is located in a spectral position which is a compromise of a blue shift and a red shift.[16,25,26,39−42,53]

In the case of a simple polarization due to the electric field generated by a coordinatively unsaturated cation (as described in point i), as well as in the case of either non-*d* or *d^0* metal cations involving a plain σ-coordination (as described in point ii), a correlation does exist between the blue-shift of the stretching frequency ($\Delta\tilde{\nu}_{CO}$) and the adsorption enthalpy $-\Delta_{ads}H$. A wide literature concerning a number of coordinatively unsaturated metal cations either exposed at the surface of oxides, or dispersed as charge-balancing cations in zeolites confirms this relationship.[62,63,67−69] It is worth of noting that the bonding features of such metal carbonyl species formed in heterogeneous conditions match with the definition of "nonclassical metal carbonyls", reported in refs 39−42 for complexes formed in homogeneous conditions. Indeed, for the species categorized as nonclassical metal carbonyls the basic "classical" metal carbonyls statement "$\tilde{\nu}_{CO}$ must be lower than 2143 cm^{-1}" does not apply.

As a conclusion, for CO ligands bound to *d*-metal cations, the experimentally observed $\tilde{\nu}_{CO}$ gives an indication of the relative contribution of the different components. In the classical metal carbonyls the effect described in point (iii) prevails, whereas in the nonclassical carbonyls the effects described in points (i) and (ii) are predominant. The predominance of the effects described in points (i) and (ii) seems to be the case of carbonyl species formed at the Cu(I) (or Ag(I)) sites located in the zeolite nanocavities, in that the $\tilde{\nu}_{CO}$ values are higher than 2143 cm^{-1}. This fact is in good agreement with the homogeneous chemistry of Cu(I) and Ag(I) ions, which are able to form carbonyl species categorized as nonclassical carbonyls possessing in most cases a relative stability.[36−42,53,58]

4.2. On the Interaction between CO/ Cu(I) and CO/Ag(I) in the Zeolite Cavities. In the present work the interaction of CO at room temperature with Cu(I)− and Ag(I)−ZSM-5 systems has been studied with the aim of elucidating the nature and the stability of the carbonyl-like bond of the adspecies. The two heterogeneous systems studied involve two *d*-block metal cations, which exhibit the same external electronic structure and which are known for their ability to form, in homogeneous chemistry, nonclassical carbonyl species of different stability.[36−42]

To compare the features of the two different counterions, it was necessary to deal with extremely well-defined systems. Care was taken to fulfill the following four requirements which allow our materials to be considered as model solids, as listed in the Introduction.[11−22,58,85] (i) Achievement of a stoichiometric ion exchange: partial exchange would result in nondesired H$^+$ counterions affecting both IR-spectroscopic and microcalorimetric data, while an overexchange would result in a heterogeneous distribution of the metal (cations) species hosted in the zeolite pores, giving rise to intrinsically difficult to interpret EXAFS, XANES, IR and microcalorimetric data. (ii) The presence of a virtually single oxidation state for the metal cation (i.e., absence of Cu(II), and clustered Ag(0) species). (iii) The knowledge of the metal site type and distribution (two nearly equipopulated families of sites: 2- and 3-fold coordinated with framework oxygen atoms). (iv) The isolated nature of the metal centers, guaranteed by the high Si/Al ratio and by the absence

of over-exchange or of clustering for Cu- and Ag−ZSM-5, respectively.

Our EXAFS results have demonstrated that Cu(I) and Ag(I) occupy the same cationic sites in ZSM-5, a fact of greatest relevance when comparing spectroscopic and thermodynamic data for the two systems. Owing to the fact the Na$^+$ and K$^+$ cations have virtually the same radii and the same charge as Cu(I) and Ag(I) respectively, we will assume that their distribution inside the zeolite channels is the same as for the noble metal cations.

Besides the overall similarity of the two systems, remarkable differences in both the spectroscopic and thermodynamic features have been observed. The spectral position of the CO stretching band of the monocarbonyl complex is blue-shifted with respect to the gas of a greater extent in the case of Ag(I) ($\Delta\tilde{\nu} = +49$ cm^{-1}) than in the case of Cu(I) ($\Delta\tilde{\nu} = +14$ cm^{-1}), see Table 2, opposite to what expected on the basis of either the sole electrostatic field or the combination of the electrostatic plus the σ-coordination effects, larger in the case of Cu(I) species. Indeed, notwithstanding the greater $\Delta\tilde{\nu}$, the zero-coverage enthalpy of adsorption, $(-\Delta_{ads}H)_0$, for [Cu(CO)]$^+$ is greater than that of [Ag(CO)]$^+$: ~120 versus ~100 kJ/mol. These facts suggest that the interpretation of the spectral position of the C−O stretching mode in the present cases requires a careful evaluation of the different contributions to the bonding.

To evaluate the electrostatic contribution in the case of Cu-(I) and Ag(I), the interaction of CO with alkaline iso-radial cations (Na$^+$ and K$^+$ respectively) hosted in the same microporous MFI system was investigated. The pure electrostatic interaction between either Na$^+$ or K$^+$ cations is characterized by the following features. (i) The stretching frequency is upward shifted at values higher than 2143 cm^{-1}, at an extent proportional to $(R_{cation} + R_{CO})^{-2}$; see refs 60 and 61a. (ii) The CO species formed are completely labile upon outgassing at room temperature, according to the very low energy of interaction ($-\Delta_{ads}H$ ~35 and ~28 kJ/mol for Na- and K−ZSM-5, respectively, see Table 2). (iii) At $p_{CO} = 90$ Torr, only a fraction of the metal cations present in the zeolite pores are able to bind CO at *RT*, according to the eq 2, which is shifted to the left:

$$M^+_{(surf)} + CO_{(gas)} \rightleftharpoons [M(CO)]^+_{(surf)} \quad (M^+ = Na^+ \text{ or } K^+) \quad (2)$$
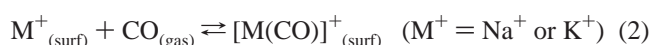
The whole set of data summarized in Table 2 allows a comparison between the different pairs of cations to be made, and namely: Na$^+$ and K$^+$; Cu(I) and Na$^+$; Ag(I) and K$^+$; and Cu(I) and Ag(I). The comparison between the two alkali-metal cations is straightforward: the volumetric data show (at $p_{CO} = 90$ Torr) that the number of CO molecules adsorbed per Na$^+$ cation is 4 times the number of CO molecules adsorbed per K$^+$ cation, in good agreement with the ration between the two equilibrium constants.[84] Moreover at the same p_{CO} the [M(CO)]$^+_{(surf)}$/M$^+_{(surf)}$ ratio is 0.67 and 0.11 for M$^+$ = Na$^+$ and K$^+$, respectively. These figures well agree with $-\Delta_{ads}H$ and $\Delta\tilde{\nu}_{CO}$ values, which are larger for the Na$^+\cdots$CO adducts, according to the pure electrostatic interaction model. The same conclusions do not hold when comparing Na$^+$ with Cu(I). Although (i) the electrostatic contribution is virtually the same for the two metal cations and (ii) in the case of copper a σ-donation contribution should determine a further increase of the blue shift, the $\tilde{\nu}_{CO}$ value for Cu(CO)$^+$ species (2157 cm^{-1}) is considerably lower than that for Na$^+\cdots$CO adduct (2178 cm^{-1}). This is a clear indication of the onset of a π-back-donation contribution. This effect is confirmed by the large value of the $(-\Delta_{ads}H)_0$ in the case of Cu(I) with respect to Na$^+$ (~120 vs 35 kJ/mol). Moving to the two other isoradial cations (Ag(I)

Heterogeneous Nonclassical Carbonyls

J. Phys. Chem. B, Vol. 108, No. 28, 2004 **9979**

and K^+), it is clearly evident that the $\Delta\tilde{\nu}_{CO}$ for silver is much larger than for K^+. This datum, which is supported also by a larger enthalpy of adsorption for Ag(I) with respect to K^+ ($\sim$100 vs 28 kJ/mol), does indicate that a σ-coordination contribution is certainly operative in the case of the transition metal cation. This fact, however, does not allow per se to discard or to accept the contribution of π-back-donation in the formation of the Ag(I)−CO bond. The answer can be found by comparing the Ag(I) data with a larger set of non-*d* and *d* systems (vide infra section 4.3).

By comparing the Cu(I) and Ag(I) cases it is worth recalling that, on the basis of the electrostatic component only, a larger $\Delta\tilde{\nu}_{CO}$ should be expected for the [Cu(CO)]$^+$ complex. However, being the experimental $\Delta\tilde{\nu}_{CO}$ much larger for [Ag(CO)]$^+$ than for [Cu(CO)]$^+$ ($+49$ vs $+14$ cm^{-1}), a stronger π-back-donation contribution must be invoked for the latter. This suggestion is in agreement also with volumetric and calorimetric data, that indicate a stronger and more extended CO interaction for Cu(I) sites than for Ag(I). However, again nothing can be said on the relative strength of the σ-donation part of the net bond between the two systems. The data reported in Table 2 are insufficient to give a firm answer to this open question. Only by comparing the spectroscopic and calorimetric data reported in the present work with the correspondent values collected on a large number of carbonyl complexes allows to attempt to do it, as will be extensively discussed in section 4.3.

By considering the evolution of the $q^{diff} = -\Delta_{ads}H$ versus CO coverage (Figure 4), the different behavior of transition- and alkali-metal cations is striking for both the heat values and the coverage reached at any p_{CO}, according to the different nature of the interaction. The heat of adsorption of the reversible component of the process (second run adsorption) for both Cu(I)− and Ag(I)−zeolites is definitely lower with respect to that measured in the first run isotherms (compare open and full symbols in Figure 4). This holds in the whole range of coverage examined and ranges in the 90−30 kJ/mol interval. In the case of Cu(I) sites the reversible adsorption corresponds to the formation of either low-energetic mono-carbonyl species, or di-carbonyl complexes through the addition of a second CO ligand, according to the following equilibriums:

$$Cu^+_{(surf)} + CO_{(gas)} \rightleftarrows [Cu(CO)]^+_{(surf)} + CO_{(gas)} \rightleftarrows$$
$$[Cu(CO_2)]^+_{(surf)} \quad (3)$$
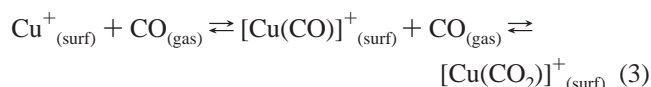
Conversely, in the case of Ag(I) sites the reversible adsorption corresponds only to the formation of labile mono-carbonyl species characterized by lower $|\Delta H_{asd}|$:

$$Ag^+_{(surf)} + CO_{(gas)} \rightleftarrows [Ag(CO)]^+_{(surf)} \quad (4)$$

The combined use of IR and microcalorimetric data allowed to discriminate the adducts formed on the basis of their relative stability. In particular, it was observed that only less than 1.5 molecules of CO per Cu(I) cation are desorbed by outgassing in relatively mild conditions (303 K and residual $p_{CO} \approx 10^{-5}$ Torr). The IR evidence indicates that in these conditions the dicarbonyl species are completely destroyed, whereas the monocarbonyl species only partially. From an energetic point of view, it is not possible to definitely single out the heat evolved during the addition of the second CO ligand from the heat evolved for the formation of the labile mono-carbonyl species. In fact the heat of adsorption curves decrease continuously without indicating sharply the saturation of one species and the starting up of the other, opposite to what observed in the case

of the interaction of Cu(I) and Ag(I) species with a ligand as strong as NH$_3$.[18,21] Nevertheless, we can tentatively assign the higher values of the heat of adsorption to the formation of the (most energetic) monocarbonyl species, thanks to the IR spectroscopy indication that the dicarbonyl species start to form when the mono-carbonyl peak does not significantly increase anymore (Figure 1a).

In the case of Cu(I)−ZSM-5, the fraction of CO molecules irreversibly adsorbed on Cu(I) (characterized by $q^{diff} = -\Delta_{ads}H$ values higher than 90 kJ/mol) is $\sim$20% of the total molecules adsorbed at $p_{CO} = 90$ Torr. This figure corresponds to $\sim$ 0.4 CO molecules adsorbed per Cu(I) cation. It is worth of noticing that the number of CO species formed at the Na$^+$ sites is also close to 0.4. This quantifies to $\sim$40% the fraction of the strongest Lewis acidic sites, which nearly corresponds to the population of the 2-fold coordinated sites evidenced by EXAFS ($\sim$50%).

The similar comparison holds for the Ag(I) and the K$^+$ systems. Also in this case, the number of K$^+$ sites able to bind CO at $p_{CO} = 90$ Torr is very close to the number of sites on which CO is irreversibly bound to Ag(I), i.e., $\sim$0.1 (see Table 2).

A separate discussion is needed in the case of the adsorption of CO on the relatively stable [Cu(NH$_3$)$_n$]$^+$ species (with $n = 1, 2$). It was found that the weakly basic CO ligand is not able to displace the irreversibly adsorbed ammonia[16,18,21] and that mixed amino−carbonyl complexes are formed, see Figure 5b. One molecule of CO per Cu(I) cation was found to be inserted in the stable amino complexes (Table 2). The differential heat of adsorption values indicate that the presence of amino-complexes in the zeolite cavities dramatically decreases (with respect to the virgin Cu(I)−ZSM-5) not only CO uptake but also the heat of formation of the CO adducts. The presence of NH$_3$, acting as a charge-releasing moiety on the Cu(I) cations, significantly decreases both the coordinative unsaturation and the actual charge of the cations (i.e., their Lewis acidity), resulting in a decrease of the net enthalpy of adsorption. The charge release is monitored by IR and XANES spectroscopy too, as reported in parts b and c of Figure 5, respectively. The former reveals a considerable downward shift of the $\tilde{\nu}_{CO}$ band (-60 cm^{-1}) by moving from [Cu(CO)]$^+$ to [Cu(NH$_3$)$_n$CO]$^+$. XANES reveals a red shift of about 2.5 eV of the edge by moving from the bare Cu(I) to [Cu(NH$_3$)$_n$CO]$^+$ complex, accompanied by a splitting of the 1s → 4p$_{xy}$ into 1s → 4p$_x$ and 1s → 4 p$_y$ components (p$_x$/p$_y$ splitting of 2.2 eV), similar to that found in the formation of low symmetric [Cu(NO)$_2$]$^+$ complexes.[9,22,23] The XANES study indicates that, not only the electrostatic component of Cu(I)−CO bond is affected by the presence of ammonia, but also σ-donation and π-back-donation contributions are modified as a consequence of the electronic rearrangements of Cu(I) in the [Cu(NH$_3$)$_n$CO]$^+$ complex. These considerations are in good agreement with the strong downward shift of the $\tilde{\nu}_{CO}$ (well lower than that of the gas) indicating that a significant π-back-donation is still operative in the formation of mixed carbonyl adducts. However, the lack of stability of the mixed amino-carbonyl species (CO ligands being readily evacuated at RT) together with the very low enthalpy of insertion of CO in the copper-amino complexes, suggests a dramatic reduction of both electrostatic and σ-donation contributions to the Cu(I)−CO bond. The investigation of the mixed amino− carbonyl complex features has thus allowed to highlight the major role of both electrostatic and σ-donation contributions into the stabilization of the carbonyl bond.

4.3. Correlation between Thermodynamic ($-\Delta_{ads}H$) and IR-Spectroscopic ($\Delta\tilde{\nu}_{CO}$) Quantities. In Figure 6 the shift of

9980 *J. Phys. Chem. B, Vol. 108, No. 28, 2004*

Bolis et al.
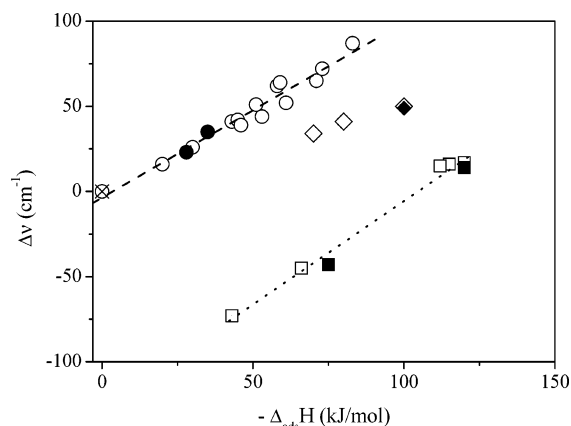
Figure 6. $\Delta\tilde{\nu}_{CO}$ ($\tilde{\nu}_{COads} - \tilde{\nu}_{COgas}$) vs $-\Delta_{ads}H$ for CO adsorbed on metal cations exposed at the surface of either microporous or nonporous systems: solid symbols refer to present work data, whereas open symbols to literature data, see Table 3 for details. Circles, *non-d/d⁰/d¹⁰* cations; squares, copper−carbonyls; diamonds, silver−carbonyls.

the stretching frequency, $\Delta\tilde{\nu}_{CO}$, is reported as a function of the enthalpy of adsorption $-\Delta_{ads}H$ for the systems investigated in the present work (full symbols) as well as for a number of systems reported in the literature (open symbols);[67] see Table 3 for quantitative values. Figure 6 and Table 3 summarize a large number of pairs of experimental data, where $\Delta\tilde{\nu}_{CO}$ and $-\Delta_{ads}H$ values have been obtained through parallel experiments carried out on samples in comparable conditions in different laboratories. The reported data can be divided into three subgroups: (i) non-*d/d⁰/d¹⁰* metal carbonyls (circles); (ii) copper metal carbonyls (squares); (iii) silver carbonyls (diamonds).

As far as non-*d/d⁰/d¹⁰* metal carbonyls are concerned, a linear correlation between the spectroscopic and thermodynamic quantities is evident, resulting in

$$\Delta\tilde{\nu}_{CO} = [(1.03 \pm 0.05)\ \text{cm}^{-1}\ \text{mol}\ (\text{kJ})^{-1}]|\Delta_{ads}H| + (-4 \pm 3)\ \text{cm}^{-1} \quad (5)$$

with $R = 0.981$. For non-*d/d⁰* metal cations any contribution of π-back-donation is prevented, while this does not necessarily hold for d^{10} metals. Among the reported data, Zn^{2+} is the only example of d^{10} metal cation and behaves as non-*d* cases both when hosted in Y-zeolite cages or exposed at the surface of ZnO. Being the linearity observed in Figure 6 on the basis of a statistically significant number of pairs of experimental data, eq 5 can be considered as an empirical rule of general validity for all non-*d/d⁰* metal−carbonyl complexes, allowing to infer calorimetric values from spectroscopic experiments and vice versa. The observed linearity implies that, when the polarization of the CO molecule and/or the σ-coordinative capacity of the cation increases (as witnessed by the increasing $\Delta\tilde{\nu}_{CO}$),[86] also the strength of the interaction increases (as testified by the increase of $-\Delta_{ads}H$). Thus either $\Delta\tilde{\nu}_{CO}$ or $-\Delta_{ads}H$ measurements can be used to evaluate the Lewis acidic strength of coordinatively unsaturated non-*d/d⁰* cationic sites. The pairs of values obtained in the present work for Na− and K−ZSM-5 (solid circles) do fit very well with the literature data, as expected.

As far as the second and third subgroups are concerned, spectroscopic and calorimetric data obtained on copper and silver carbonyls lie in a completely different region of the $-\Delta_{ads}H/\Delta\tilde{\nu}_{CO}$ plane (Figure 6). This means that in the *d*-block metals case the spectroscopic and thermodynamic parameters do not correlate with the empirical rule reported in eq 5. The interaction between the CO ligands and the metal transition

TABLE 3: Enthalpy changes ($q^{\text{diff}} = -\Delta_{ads}H$) in the Zero-Coverage Limit and C−O Stretching Frequencies Shift ($\Delta\tilde{\nu}_{CO}$) for CO Adsorbed on Metal Cations Systems Reported in Figure 6 (See the Fifth Column for the Adopted Symbols: NR = Not Reported in the Figure)[a]

system	$-\Delta H_{ads}$ (kJ mol⁻¹)	$\Delta\tilde{\nu}_{CO}$ (cm⁻¹)	ref	symbol
CO_{gas}	0	0	90	⊗
NaCl	20	16	91	○
K^+−ZSM-5	28	23	this work	●
Na^+−Y	24	26	92	○
Na^+−ZSM-5	28	33	62	○
Na^+−Y	30	26	67c	○
Li^+-doped Al_2O_3	30	37	93	○
Ba^{2+}−Y	35	24	92	○
Na^+−ZSM-5	35	32	49	○
Na^+−ZSM-5	35	35	this work	●
Ca^{2+}−Y	45	42	92	○
Ce^{2+}-doped Al_2O_3	43	41	67e	○
Ca^{2+}-doped Al_2O_3	45	42	67f	○
ZnO	46	39	67c	○
Ca^{2+}−Y	51	51	67c	○
TiO_2 (site ◇)[b]	53	44	67b	○
Al_2O_3 (site A)[b]	58	62	67f	○
Zn^{2+}−Y	59	64	67c	○
TiO_2 (site ◇)[b]	61	52	67b	○
Zn^{2+}−Y	71	64	92	○
TiO_2 (site ◈)[b]	71	65	67b	○
Al_2O_3 (site B)[b]	73	72	67f	○
Al_2O_3 (site C)[b]	83	87	67f	○
Cu(I)−ZSM-5	120	14	this work	■
Cu^+−ZSM-5	91	16	49	NR
Cu^+−ZSM-5	82	6	49	NR
Cu^+−ZSM-5	70	−7	49	NR
Cu^+−ZSM-5	120	16	6,53	□
Cu^+−ZSM-5	100	8	6,53	NR
Cu^+−ZSM-5	70	-8	53	NR
Cu^+/SiO_2·Al_2O_3	115	16	53	□
Cu^+/SiO_2·Al_2O_3	112	15	53	□
$[Cu(NH_3)_n]^+$−ZSM-5	75	−43	this work	■
Cu^+/ZnO	66	−45	88	□
Cu^0/ZnO	43	−74	88	□
Ag(I)−ZSM-5	100	49	this work	◆
$(Ag^+)_{2-fold}$−ZSM-5	100	50	53	◇
Ag^+−SiO_2·Al_2O_3	100	50	53	◇
Ag^+−SiO_2	70	34	53	◇
$(Ag^+)_{3-fold}$−ZSM-5	80	41	53	◇

[a] First set of data refers to d^0, d^{10} or non−d metals, whereas the second and third sets to copper and silver carbonyls, respectively. [b] For the definition of the surface site, see the corresponding reference.

cations is indeed much more complex than the one involving non-*d/ d⁰/d¹⁰* metal cations, in that a π-back-donation is, at least partially, always operative. The π-back-donation contribution is however larger for copper than for silver, as indicated by the larger deviation from the empirical line 5 of the former values. To attempt to single out the different π- and σ-contributions, it is useful to analyze in details the different pairs of values reported in Table 3. The pair of values ($-\Delta_{ads}H = 120$ kJ mol⁻¹ and $\Delta\tilde{\nu}_{CO} = -17$ cm⁻¹) obtained for the Cu(I)−ZSM-5 model system reported in the present work corresponds unambiguously to the formation of well defined $[Cu(CO)]^+$ complexes. This pair of values well agrees with those reported by Kuroda et al.[53] on Cu/SiO_2·Al_2O_3. Conversely, a straightforward comparison with the values reported by the Kuroda group on the Cu−ZSM-5 systems is hardly feasible. In fact the Kuroda's group has reported various values for a number of different copper-exchanged zeolites, prepared following different wet exchange procedures with Cu(II)−salts and subsequent thermal reduction to Cu(I);[49,53] see Table 3. The values reported for CO adsorbed on Cu−ZSM-5 sites vary in a widespread interval of both $\Delta\tilde{\nu}_{CO}$ (-8 to $+17$ cm⁻¹) and $-\Delta_{ads}H$ (70 to 120 kJ mol⁻¹). Among

Heterogeneous Nonclassical Carbonyls

J. Phys. Chem. B, Vol. 108, No. 28, 2004 **9981**

all the reported pairs, only one ($\Delta\tilde{\nu}_{CO}$ = +17 cm^{-1} and $-\Delta_{ads}H$ = 120 kJ mol^{-1}) agrees with the datum reported by us. The apparent disagreement between the sets of data reported by us and the Kuroda's group depends on two different kinds of reasons. First, Kuroda's laboratory samples are intrinsically more complex than our model system, in that different copper species (which relative proportion is modulated by the different exchange procedures, see the introduction) are present. Second, the spectroscopic and microcalorimetric outputs are interpreted by the two groups following a different approach. Kuroda and co-workers, associate to any resolved IR component a $-\Delta_{ads}H$ value as measured at the same p_{CO}. On the spectroscopic ground, this assignment is based on the hypothesis that any defined C−O stretching band is due to CO molecules adsorbed into different Cu(I) sites. By contrast, in our samples the IR-spectroscopic evidence did not allow to discriminate different Cu(I) sites simply on the basis of the $\tilde{\nu}_{CO}$ of the [Cu(CO)]$^+$ complex. Davidova et al.,[28] who have simulated the interaction of CO with Cu(I) species located on different cationic sites of MFI and FER zeolites by means of QM-pot code, arrived to the same conclusion. Using diffuse reflectance FTIR, Borovkov et al. analyzed fundamental, combination, and overtone vibrations of adsorbed CO and concluded that two different types of Cu(I) sites can be only hardly discriminated by IR spectroscopy.[87] As for the low p_{CO} complexes, our data agrees with those of Kuroda et al.[6,53] ($\Delta\tilde{\nu}_{CO}$ = +16 cm^{-1}; $-\Delta_{ads}H$ = 120 kJ mol^{-1}). By increasing p_{CO}, a well defined doublet develops in our IR spectra (Figure 1a) at $\Delta\tilde{\nu}_{CO}$ = +35 and +8 cm^{-1}. Similar features ($\Delta\tilde{\nu}_{CO}$ = +32 and +6 cm^{-1}) although less resolved appear in Kuroda's spectra as well. We ascribed the high p_{CO} doublet to the formation of a [Cu(CO)$_2$]$^+$ complex according to eq 3, while Kuroda et al.[6,49,53] assign the two bands to CO species physisorbed on two different copper sites. In our case, the validity of the dicarbonyl interpretation has been definitively proven by a two-dimensional IR correlation analysis (2D-COS-IR), which allowed to establish the correlation among the observed IR features (see section D of the Supporting Information). Thus, on the basis of these reasons, we have chosen to include in the data plotted in Figure 6 only the low-p_{CO} pair ($\Delta\tilde{\nu}_{CO}$ = +16 cm^{-1}; $-\Delta_{ads}H$ = 120 kJ mol^{-1}) among all $\Delta\tilde{\nu}_{CO}$, $-\Delta_{ads}H$ pairs reported by Kuroda et al.;[6,49,53] see Table 3.

The other ($\Delta\nu_{CO}$, $-\Delta_{ads}H$) pairs reported in Table 3 refer to partially reduced copper species. It has been reported (vide supra) that in the case of CO adsorbed on [Cu(NH$_3$)$_n$]$^+$ sites entrapped in the zeolite pores the CO frequency does suffer a red shift. Correspondingly, a lower enthalpy of adsorption ($-\Delta_{ads}H$ = 80 kJ/mol) with respect to the bare Cu(I) sites was measured, indicating a weakening of the interaction. Indeed, the actual charge density of the copper cations is lower in the presence of charge-releasing NH$_3$ ligands, as probed by XANES, as well; see Figure 5c. For this reason, the copper cations in our [Cu(NH$_3$)$_n$]$^+$ complexes are suspected to be at least partially reduced. To confirm this suggestion, spectroscopic and thermodynamic data on the interaction of CO with partially reduced copper species grafted on a non porous ZnO matrix[88] are reported in the diagram shown in Figure 6 (open squares). A linear correlation, which slope is close to that of eq 5 line, is empirically observed, in the 40−120 kJ mol^{-1} |$\Delta_{ads}H$| range,[89] for the reported copper carbonyls:

$$\Delta\tilde{\nu}_{CO} = [(1.21 \pm 0.07)\ \text{cm}^{-1}\ \text{mol}\ (\text{kJ})^{-1}]\Delta_{ads}H +$$
$$(-127 \pm 6)\ \text{cm}^{-1} \quad (6)$$

with R = 0.993. The positive value of the slope [(1.21 ± 0.07)

cm^{-1} mol (kJ)$^{-1}$] of the linear correlation is surprising. Indeed, as far as classical carbonyls are concerned,[39−42] an increase of the π-back-donation is accompanied by a decrease of the IR-spectroscopic shift and by a parallel enhancement of the M$^+$−C bond strength: this should imply a negative slope in the $-\Delta_{ads}H/\Delta\tilde{\nu}_{CO}$ plane. An explanation of the copper carbonyl data reported in Figure 6 (open and full squares) is the following. The linear decrease of $\Delta\tilde{\nu}_{CO}$ observed by moving from [Cu(CO)]$^+$ through [Cu(NH$_3$)$_n$CO]$^+$ and Cu(I)/ZnO down to Cu(0)/ZnO is not due to a progressive increase of the π-back-donation component of the Cu−CO bond, but to a progressive decrease of the net charge on the Cu(I) cations. This brings about to a progressive extinguishment of the electrostatic component. This hypothesis explains why $\Delta\tilde{\nu}_{CO}$ and $-\Delta_{ads}H$ correlate positively and why the slope obtained in eq 6 is similar to that obtained for non-d/d^0 system. The decrease of the net charge on the cation in the [Cu(NH$_3$)$_n$CO]$^+$ system, with respect to the pure carbonyl adduct, is justified by the charge-releasing role played by ammonia ligands, whereas the effect observed on the Cu(I)/ZnO and Cu(0)/ZnO systems has been caused by progressive reducing treatments in H$_2$.[88]

As for silver carbonyls, thanks to the same preparation procedure adopted, comparable systems have been investigated by us and by Kuroda's group.[53] Thus, our results are in perfect agreement with those reported by Kuroda's group for CO adsorbed on Ag(I) sites located on either ZSM-5 or SiO$_2$·Al$_2$O$_3$ matrixes. Conversely, lower $\Delta\tilde{\nu}_{CO}$ and $-\Delta_{ads}H$ were measured for Ag(I) sites hosted on a SiO$_2$ matrix (see Table 3). Due to the limited number of calorimetric and spectroscopic pairs available for Ag carbonyls, it has not been possible to draw a correlation relationship between $\Delta\tilde{\nu}_{CO}$ and $-\Delta_{ads}H$ values, as was done in the case of both Cu and non-$d/d^0/d^{10}$ metal carbonyls (eqs 5 and 6, respectively). This is particularly true owing to the lack of experimental data related to partially reduced Ag species in the low $-\Delta_{ads}H/\Delta\tilde{\nu}_{CO}$ region.

5. Conclusions

The RT adsorption of CO on Cu(I)− and Ag(I)−ZSM-5 model systems has been studied by means of the joint use of IR spectroscopy and adsorption microcalorimetry, to describe the features of carbonyl-like species formed in the zeolite pores. It has been confirmed that CO binds to the d-block metal cations through a chemical interaction which involves an enthalpy change of ∼120 and ∼100 kJ/mol for Cu(I) and Ag(I) sites, respectively. The spectral position of the CO bands ($\tilde{\nu}_{CO}$ > 2143 cm^{-1}) alone does not allow to assess whether, further to a σ-coordination of the CO lone pair; also a π-back-donation is operative in the carbonyl bond stabilization. Substantial evidence arose by comparing the C−O stretching frequencies of the carbonyl species formed in the various systems investigated (including the electrostatic adducts formed at the Na$^+$ and K$^+$ sites located in the pores of ZSM-5 zeolite, especially exchanged for comparison purposes). The $\Delta\tilde{\nu}_{CO}$ shifts measured in the present work have been plotted against the correspondent $-\Delta_{ads}H$ enthalpies of adsorption, and have been compared with a large set of non-$d/d^0/d^{10}$ metal carbonyls values reported in the literature. Five major points have been assessed.

(i) In the case of both Cu(I) and Ag(I) d-block metal cations, even if the carbonyl species must be categorized as nonclassical carbonyls, a significant π-back-donation does contribute to the stabilization of the carbonyl bond. This is witnessed on one hand by the enhancement of the energy of interaction with respect to a plain σ-coordination, and on the other hand by the stability of a fraction of Cu(I)−and Ag(I)−carbonyls which resist to a prolonged outgassing.

(ii) A difference in stability has been observed between Cu(I)−and Ag(I)−carbonyls, in that both the heat of formation ($-\Delta_{ads}H$) and the population of stable carbonyls are larger for Cu(I) than for Ag(I) species, according to the larger extent of the π-back-donation for the former.

(iii) An empirical rule (already reported by some of us in refs 65, 67f, and here resumed and extended) linearly correlates $\Delta\tilde{\nu}_{CO}$ and $-\Delta_{ads}H$ quantities for non-d/d^0 metal−carbonyls. This rule is of general validity in that allows to infer in the case of non-d/d^0 metal carbonyls the enthalpy values from IR-spectroscopic experiments, and vice versa. Conversely, as far as d-block metal cations are concerned, the extent of the π-back-donation component can be roughly estimated by the deviation from the empirical rule

(iv) In the case of copper species, it has been observed that as far as the actual charge of Cu cations decreases (either because of the presence of charge-releasing ligands in mixed complexes, or because of thermal treatments in reducing atmosphere), the strength of the carbonyl bond dramatically decreases. This is demonstrated by the lower enthalpy of adsorption of CO (with respect to the formation of monocarbonyl complexes on the pristine Cu(I) sites) and by the lack of stability of the CO species upon outgassing. Being the spectral position of the IR band in the case of such labile species typical of metal carbonyls involving π-back-donation ($\tilde{\nu}_{CO} < 2143$ cm^{-1}) the instability of the carbonyl adducts is interpreted as due to the lack of a strong electrostatic and σ-coordinative contributions in the formation of (partially)-reduced copper−carbonyls. The idea, generally accepted, that π-back-donation gives a major contribution in the stabilization of the carbonyl bond has been here criticized.

(v) A linear correlation between $\Delta\tilde{\nu}_{CO}$ and $-\Delta_{ads}H$ has been found for the different Cu-species reported, the slope of which is positive and close to that of the empirical rule line reported for non-d/d^0 metal carbonyls.

Supporting Information Available: Descriptions of the local environment of metal sites as probed by EXAFS, the structure of [Cu(CO)$_2$]$^+$ complexes, calorimetric isotherms, and interpretation of IR spectra. This material is available free of charge via the Internet at http://pubs.acs.org.

References and Notes

(1) (a) Iwamoto, M.; Yahiro, H.; Mizuno, N.; Zhang, W. X.; Mine, Y.; Furukawa, H.; Kagawa, S. *J. Phys. Chem.* **1992**, *96*, 9360−9366. (b) Sato, S.; Yoshihiro, Y.; Yahiro, H.; Mizuno, N.; Iwamoto, M. *Appl. Catal.* **1991**, *70*, L1-L5.

(2) (a) Li, Y. K.; Hall, W. K. *J. Phys. Chem.* **1990**, *94*, 6145−6148. (b) Li, Y. K.; Hall, W. K. *J. Catal.* **1991**, *129*, 202−215. (c) Smits, R. H. H.; Iwasawa, Y. *Appl. Catal. B-Environ.* **1995**, *6*, L201-L207.

(3) Shelef, M. *Chem. Rev.* **1995**, *95*, 209−225 and references therein.

(4) Following the convention introduced by Iwamoto, a 100% exchange is reached when a Cu(II) cation is introduced for each two monovalent counterions, i.e., for each two Al(III) species of the framework.

(5) (a) Wichterlova, B.; Dedecek, J.; Vondrova, A. *J. Phys. Chem.* **1995**, *99*, 1065−1067. (b) Dedecek, J.; Sobalik, Z.; Tvaruzkova, Z.; Kaucky, D.; Wichterlova, B. *J. Phys. Chem.* **1995**, *99*, 16327−16337.

(6) Kumashiro, P.; Kuroda, Y.; Nagao, M. *J. Phys. Chem. B* **1999**, *103*, 89−96, see also additional information.

(7) Grünert, W.; Hayes, N. W.; Joyner, R. W.; Shapiro, E. S.; Rafiq, M.; Siddiqui, H.; Baeva, G. N. *J. Phys. Chem.* **1994**, *98*, 10832−10846.

(8) Turnes Palomino, G.; Fisicaro, P.; Bordiga, S.; Zecchina, A.; Giamello, E.; Lamberti, C. *J. Phys. Chem. B* **2000**, *104*, 4064−4073.

(9) Llabrés i Xamena, F. X.; Fisicaro, P.; Berlier, G.; Zecchina, A.; Turnes Palomino, G.; Prestipino, C.; Bordiga, S.; Giamello, E.; Lamberti, C. *J. Phys. Chem. B* **2003**, *107*, 7036−7044.

(10) Gervasini, A.; Picciau, C.; Auroux, A. *Microporous Mesoporous Mater.* **2000**, *35−36*, 457−469.

(11) Spoto, G.; Bordiga, S.; Scarano, D.; Zecchina, A. *Catal. Lett.* **1992**, *13*, 39−44.

(12) Spoto, G.; Zecchina, A.; Bordiga, S.; Ricchiardi, G.; Martra, G.; Leofanti, G.; Petrini, G.; *Appl. Catal. B* **1994**, *3*, 151−172.

(13) Spoto, G.; Bordiga, S.; Ricchiardi, G.; Scarano, D.; Zecchina, A.; Geobaldo, F. *J. Chem. Soc., Faraday Trans.* **1995**, *91*, 3285−3290.

(14) Lamberti, C.; Bordiga, S.; Salvalaggio, M.; Spoto, G.; Zecchina, A.; Geobaldo, F.; Vlaic, G.; Bellatreccia, M. *J. Phys. Chem. B* **1997**, *101*, 344−360, references therein.

(15) Zecchina, A.; Bordiga, S.; Salvalaggio, M.; Spoto, G.; Scarano, D.; Lamberti, C. *J. Catal.* **1998**, *173*, 540−542.

(16) Zecchina, A.; Bordiga, S.; Turnes Palomino, G.; Scarano, D.; Lamberti, C.; Salvalaggio, M. *J. Phys. Chem. B* **1999**, *103*, 3833−3844.

(17) Lamberti, C.; Turnes Palomino, G.; Bordiga, S.; Berlier, G.; D'Acapito, F.; Zecchina, A. *Angew. Chem., Int. Ed. Engl.* **2000**, *39*, 2138−2141.

(18) Bolis, V.; Maggiorini, S.; Meda, L.; D'Acapito, F.; Turnes Palomino, G.; Bordiga, S.; Lamberti, C. *J. Chem. Phys.* **2000**, *113,* 9248−9261.

(19) Bolis, V.; Bordiga, S.; Graneris, V.; Lamberti, C.; Turnes Palomino, G.; Zecchina, A. *Stud. Surf. Sci. Catal.* **2000**, *130*, 3261−3266.

(20) Turnes Palomino, G.; Zecchina, A.; Giamello, E.; Fisicaro, P.; Berlier, G.; Lamberti, C.; Bordiga, S. *Stud. Surf. Sci. Catal.* **2000**, *130*, 2915−2920.

(21) Bolis, V.; Bordiga, S.; Turnes Palomino, G.; Zecchina, A.; Lamberti, C. *Thermochim. Acta* **2001**, *397*, 131−145.

(22) Prestipino, C.; Berlier, G.; Llabrés i Xamena, F. X.; Spoto, G.; Bordiga, S.; Zecchina, A.; Turnes Palomino, G.; Yamamoto, T.; Lamberti, C. *Chem. Phys. Lett.* **2002**, *363*, 389−396.

(23) Lamberti, C.; Bordiga, S.; Bonino, F.; Prestipino, C.; Berlier, G.; Capello, L.; D'Acapito, F.; Llabrés i Xamena, F. X.; Zecchina, A. *Phys. Chem. Chem. Phys.* **2003**, *5*, 4502−4509.

(24) Rodriguez-Santiago, L.; Sierka, M.; Branchadell, V.; Sodupe, M.; Sauer, J. *J. Am. Chem. Soc.* **1998**, *120*, 1545.

(25) (a) Nachtigallova, D.; Nachtigall, P.; Sierka, M.; Sauer, J. *Phys. Chem. Chem. Phys.* **1999**, *1*, 2019. (b) Nachtigallova, D.; Nachtigall, P.; Sauer, J. *Phys. Chem. Chem. Phys.* **2001**, *3*, 1552.

(26) (a) Nachtigall, P.; Nachtigallova, D.; Sauer, J. *J. Phys. Chem. B* **2000**, *104*, 1738. (b) Nachtigall, P.; Davidova, M.; Nachtigallova, D. *J. Phys. Chem. B* **2001**, *105*, 3510.

(27) Spuhler, P.; Holthausen, M. C.; Nachtigallova, D.; Nachtigall, P.; Sauer, J. *Chem. Euro. J.* **2002**, *8*, 2099−2115.

(28) Davidova, M.; Nachtigallova, D.; Bulanek, R.; Nachtigall, P. *J. Phys. Chem. B* **2003**, *107*, 2327−2332.

(29) Calzaferri, G.; Leiggener, C.; Glaus, S.; Schürco, D.; Kuge, K. *Chem. Soc. Rev.* **2003**, *32*, 29−37.

(30) Lamberti, C.; Spoto, G.; Scarano, D.; Pazé, C.; Salvalaggio, M.; Bordiga, S.; Zecchina, A.; Turnes Palomino, G.; D'Acapito, F. *Chem. Phys. Lett.* **1997**, *269*, 500−508.

(31) Turnes Palomino, G.; Bordiga, S.; Zecchina, A.; Marra, G. L.; Lamberti, C. *J. Phys. Chem. B* **2000**, *104*, 8641−8651.

(32) Lamberti, C.; Bordiga, S.; Zecchina, A.; Salvalaggio, M.; Geobaldo, F.; Otero Areán, C. *J. Chem. Soc., Faraday Trans.* **1998**, *94*, 1519−1525.

(33) (a) Yamaguchi, A.; Shido, T.; Inada, Y.; Kogure, T.; Asakura, K.; Nomura, M.; Iwasawa, Y. *Bull. Chem. Soc. Jpn.* **2001**, *74*, 801−808. (b) Shido, T.; Yamaguchi, A.; Inada, Y.; Asakura, K.; Nomura, M.; Iwasawa, Y. *Topics Catal.* **2002**, *18*, 53−58.

(34) Ozin, A.; Kuperman, A.; Stein, A. *Angew. Chem., Int. Ed. Engl.* **1989**, *28*, 359.

(35) Bein, T.; Enzel, P. *Angew. Chem., Int. Ed. Engl.* **1989**, *28*, 1692.

(36) Hurlburt, P. K.; Rack, J. J.; Dec, S. F.; Anderson, O. P.; Strauss, S. H. *Inorg. Chem.* **1993**, *32*, 373−374.

(37) Hurlburt, P. K.; Rack, J. J.; Luck, J. S.; Dec, S. F.; Webb, J. D.; Anderson, O. P.; Strauss, S. H. *J. Am. Chem. Soc.* **1994**, *116*, 10003−10014.

(38) Tsumori, N.; Xu, Q.; Hirahara, M.; Tanihata, S.; Souma, Y.; Nishimura, Y.; Kuriyama, N.; Tsubota, S. *Bull. Chem. Soc. Jpn.* **2002**, *75*, 2257−2268.

(39) Willner, H.; Aubke, F. *Angew. Chem., Int. Ed. Engl.* **1997**, *36*, 2403−2425, and references therein.

(40) Lupinetti, A. J.; Strauss, S. H.; Frenking, G. *Prog. Inorg. Chem.* **2001**, *49*, 1−112, and references therein.

(41) Strauss, S. H. *J. Chem. Soc., Dalton Trans*. **2000**, 1−6, and references therein.

(42) Xu, Q. *Coord. Chem. Rev.* **2002**, *231*, 83−108, and references therein.

(43) Kuroda, Y.; Kotani, A.; Maeda, H.; Moriwaki, H.; Morimato, T.; Nagao, M. *J. Chem. Soc., Faraday Trans.* **1992**, *88*, 1583−1590.

(44) Kuroda, Y.; Yoshikawa, Y.; Emura, S.; Kumashiro, R.; Nagao, M. *J. Phys. Chem. B* **1999**, *103*, 2155−2164.

(45) Kuroda, Y.; Kumashiro, R.; Itadani, A.; Nagao, M.; Kobayashi, H. *Phys. Chem. Chem. Phys.* **2001**, *3*, 1383−1390.

(46) Kuroda, Y.; Okamoto, T.; Kumashiro, R.; Yoshikawa, Y.; Nagao, M. *Chem. Commun.* **2002**, 1758−1759.

(47) Iwamoto, M.; Hoshino, Y. *Inorg. Chem.* **1996**, *35*, 6918−6921.

(48) (a) Hadjiivanov, K. I.; Kantcheva, M. M.; Klissurski, D. G. *J. Chem. Soc., Faraday Trans.* **1996**, *92* 4595−4600. (b) Hadjiivanov, K. I. *Microporous Mesoporous Mater.* **1998**, *24*, 41−49. (c) Hadjiivanov, K. I.; Dimitrov, L. *Microporous Mesoporous Mater.* **1999**, *27*, 49−56.

(49) Kuroda, Y.; Yoshikawa, Y.; Kumashiro, R.; Nagao, M. *J. Phys. Chem. B* **1997**, *101*, 6497−6503.

(50) Very recently Kuroda's group has reported XAS and IR data on a Cu−ZSM-5 prepared according to our procedure (Kuroda, Y.; Yagi, K.; Horiguchi, N.; Yoshikawa, Y.; Kumashiro, R.; Nagao, M. *Phys. Chem. Chem. Phys.* **2003**, *5*, 3318−3327). However, the resolution of the IR features obtained by dosing CO on a Cu−ZSM-5 sample prepared by gas-phase exchange with CuCl has not been improved with respect to what obtained by the same group in previous works.

(51) Kuroda, Y.; Kumashiro, R.; Nagao, M. *Appl. Surf. Sci.* **2002**, *196*, 408−422.

(52) Sun, T.; Seff, K. *Chem. Rev.* **1994**, *94*, 857−870, and references therein.

(53) Kuroda, Y.; Onishi, H.; Mori, T.; Yoshikawa, Y.; Kumashiro, R.; Nagao, M.; Kobayashi, H. *J. Phys. Chem. B* **2002**, *106*, 8976−8987, and references therein.

(54) Jacobs, P. A.; Uytterhoeven, J. B.; Beyer, H. K. *Chem. Commun.* **1977**, 128−129.

(55) Baba, T.; Ono, Y. *Zeolites* **1987**, *7*, 292−301.

(56) Anpo, M.; Matsuoka, M.; Yamashita, H. *Catal. Today* **1997**, *35*, 1997 177−181.

(57) Shannon, R. D. *Acta Crystallogr. A* **1976**, *32*, 751−767.

(58) Bordiga, S.; Turnes Palomino, G.; Arduino, D.; Lamberti, C.; Zecchina, A.; Otero Areán, C. *J. Mol. Catal. A* **1999**, *146*, 97−106.

(59) Hadjiivanov, K.; Knozinger, H. *J. Phys. Chem. B* **1998**, *102*, 10936−10940.

(60) (a) Bordiga, S.; Escalona Platero, E.; Otero Areán, C.; Lamberti, C.; Zecchina, A. *J. Catal.* **1992**, *137*, 179−185. (b) Zecchina, A.; Bordiga, S.; Lamberti, C.; Spoto, G.; Carnelli, L.; Otero Areán, C. *J. Phys. Chem.* **1994**, *98*, 9577−9582. (c) Bordiga, S.; Lamberti, C.; Geobaldo, F.; Zecchina, A.; Turnes Palomino, G.; Otero Areán, C. *Langmuir* **1995**, *11*, 527−533.

(61) (a) Lamberti, C.; Bordiga, S.; Geobaldo, F.; Zecchina, A.; Otero Areán, C. *J. Chem. Phys.* **1995**, *103*, 3185−3165. (b) Ferrari, A. M.; Ugliengo, P. Garrone, E. *J. Chem. Phys.* **1996**, *105*, 4129−4139. (c) Ferrari, A. M.; Neyman, K. M.; Rosch, N. *J. Phys. Chem. B* **1997**, *101*, 9292−9298.

(62) Garrone, E.; Fubini, B.; Bonelli, B.; Onida, B.; Otero Areán, C. *Phys. Chem. Chem. Phys.* **1999**, *1*, 513−518.

(63) Goldman, A. S.; Krogh-Jespersen, K. *J. Am. Chem. Soc.* **1996**, *118*, 12159−12166.

(64) Zhou, M. F.; Andrews, L.; Baushlicher, C. W. *Chem. Rev.* **2001**, *101*, 1931−1961.

(65) Zecchina, A.; Scarano, D.; Bordiga, S.; Spoto, G.; Lamberti, C. *Adv. Catal.* **2001**, *46*, 265−397.

(66) Lamberti, C.; Prestipino, C.; Bonino, F.; Capello, L.; Bordiga, S.; Spoto, G.; Zecchina, A.; Diaz Moreno, S.; Cremaschi, B.; Garilli, M.; Marsella, A.; Carmello, D.; Vidotto, S.; Leofanti, G. *Angew. Chem., Int. Ed. Engl.* **2002**, *41*, 2341−2344.

(67) (a) Morterra, C.; Garrone, E.; Bolis, V.; Fubini, B. *Spectrochim. Acta A* **1987**, *43*, 1577−1581. (b) Bolis, V.; Fubini, B.; Garrone, E.; Morterra, C. *J. Chem. Soc., Faraday Trans. 1* **1989**, *85*, 1383−1395. (c) Bolis, V.; Fubini, B.; Garrone, E.; Giamello, E.; Morterra, C. *Stud. Surf. Sci. Catal.* **1989**, *48*, 159−166. (d) Morterra, C.; Cerrato, G.; Bolis, V.; Fubini, B.; *Spectrochim. Acta A* **1993**, *49*, 1269−1288. (e) Bolis, V.; Cerrato, G.; Magnacca, G.; Morterra, C. *Thermochim. Acta* **1998**, *312*, 63−77. (f) Bolis, V.; Magnacca, G.; Morterra, C. *Res. Chem. Intermed.* **1999**, *25*, 25−56.

(68) (a) Garrone, E.; Bolis, V.; Fubini, B.; Morterra, C. *Langmuir* **1989**, *5*, 892−899. (b) Bolis, V.; Fubini, B.; Garrone, E.; Morterra, C.; Ugliengo, P. *J. Chem. Soc., Faraday Trans.* **1992**, *88*, 391−398. (c) Bolis, V.; Morterra, C.; Fubini, B.; Ugliengo, P.; Garrone, E. *Langmuir* **1993**, *9*, 349−367.

(69) Spoto, G.; Gribov, E.; Ricchiardi, G.; Damin, A.; Scarano, D.; Bordiga, S.; Lamberti, C.; Zecchina, A. *Prog. Surf. Sci.* **2004**, in press.

(70) Lamberti, C.; Prestipino, C.; Bordiga, S.; Fitch, A. N.; Marra, G. L. *Nucl. Instr. Methods B* **2003**, *200*, 155−159.

(71) Lamberti, C.; Prestipino, C.; Bordiga, S.; Berlier, G.; Spoto, G.; Zecchina, A.; Laloni, A.; La Manna, F.; Danca, F.; Felici, R.; D'Acapito, F.; Roy, P. *Nucl. Instr. Methods B* **2003**, *200*, 196−201.

(72) (a) Bolis, V.; Bordiga, S.; Lamberti, C.; Zecchina, A.; Petrini, G.; Rivetti, F.; Spanò, G. *Langmuir* **1999**, *15*, 5, 753. (b) Bordiga, S.; Roggero, I.; Ugliengo, P.; Zecchina, A.; Bolis, V.; Artioli, G.; Buzzoni, R.; Marra, G. L.; Rivetti, F.; Spanò, G.; Lamberti, C. *J. Chem. Soc., Dalton Trans.* **2000**, 3921. (c) Bolis, V.; Busco, C.; Bordiga, S.; Ugliengo, P.; Lamberti, C.; Zecchina, A. *Appl. Surf. Sci.* **2002**, *196*, 56−70.

(73) (a) Filipponi, A.; Di Cicco, A.; Natoli, C. R. *Phys. Rev. B* **1995**, *52*, 15122−15134. (b) Filipponi, A.; Di Cicco, A. *Phys. Rev. B* **1995**, *52*, 15135−15149.

(74) Della Gatta, G. *Thermochim. Acta*, **1985**, *96*, 349−363.

(75) (a) Gravelle, P. C. *Adv. Catal.* **1972**, *22*, 191−263. (b) Gravelle, P. C. *Thermochim. Acta*, **1985**, *96*, 365−376.

(76) (a) Auroux, A. In *Physical Techniques for Solid Materials*; Imelik, B., Védrine, J. C., Eds.; Plenum Press: New York, 1994. (b) Auroux, A. *Topics Catal.* **1997**, *4*, 71−77.

(77) Fubini, B. *Thermochim. Acta* **1988**, *135*, 19−29.

(78) Solinas, V.; Ferino, I. *Catal. Today* **1998**, *41*, 179−189.

(79) Cardona-Martinez, N.; Dumesic, J. *Adv. Catal.* **1992**, *38*, 149−244.

(80) Dunne, J. A.; Rao, M.; Sircar, S.; Gorte, R. J.; Myers, A. L. *Langmuir* **1996**, *12*, 5888−5895.

(81) Owing to the high dilution of cation sites in ZSM-5 (Si/Al = 14), no induced heterogeneity effects, due to lateral interaction (typical of adsorption processes on well-defined oxidic surfaces) are present.

(82) (a) Gorte, R. J.; White, D. *Microporous Mesoporous Mater.* **2000**, *35−36*, 447−455. (b) Yang, L.; Trafford, K.; Kresnawahjuesa, O.; Šepa, J.; Gorte, R. J. *J. Phys. Chem. B* **2001**, *105*, 1935−1942.

(83) Bolis, V.; Broyer, M.; Barbaglia, A.; Busco, C.; Foddanu, G. M.; Ugliengo, P. *J. Mol. Catal. A: Chem.* **2003**, *204−205*, 561−569.

(84) The equilibrium constant for CO adsorption on Na^+- and K^+ZSM-5 obtained according to the Langmuir model are 4.8×10^{-3} and 1.2×10^{-3} $Torr^{-1}$, respectively.

(85) Bordiga, S.; Lamberti, C.; Turnes Palomino, G.; Geobaldo, F.; Arduino, D.; Zecchina, A. *Microporous Mesoporous Mater.* **1999**, *30*, 129−135.

(86) Zecchina, A.; Lamberti, C.; Bordiga, S. *Catal. Today* **1998**, *41*, 169−177.

(87) Borovkov, V. Y.; Jiang, M.; Fu, Y. *J. Phys. Chem. B* **1999**, *103*, 5010−5019.

(88) Giamello, E.; Fubini, B.; Bolis, V. *Appl. Catal.* **1988**, *36,* 287−298.

(89) It is evident that eq 6 can not hold in the $\Delta_{ads}H \rightarrow 0$ limit, as a nonzero $\Delta\tilde{\nu}_{CO}$ value for the limit of not-interacting systems is not reasonable. The observed linearity has thus to be considered valid only in the $|\Delta_{ads}H|$ interval of the investigated examples, which is 40 kJ mol^{-1} < $|\Delta_{ads}H|$ < 120 40 kJ mol^{-1}. Note also that, conversely to the non-*d* and d^0 case, the $-\Delta_{ads}H \rightarrow 0$ limit has no meaning in the Cu(I) carbonyl case, as the presence of the π back-donation contribution will always guarantee a considerable $-\Delta_{ads}H$ value.

(90) Ewing, G. E. *J. Chem. Phys.* **1962**, *37*, 2250−2256.

(91) Gevirzman, R.; Kozirovski, Y.; Folman, M. *Trans. Faraday Soc.* **1969**, *65*, 2206−2214.

(92) (a) Egerton, T. A.; Stone, F. S. *Trans. Faraday Soc.* **1970**, *66*, 2364−2377. (b) Egerton, T. A.; Stone, F. S. *J. Chem. Soc., Faraday Trans. 1* **1973**, *69*, 22−38.

(93) Magnacca, G.; Morterra, C.; Bolis, V. unpublished results.